SULFATION CHARACTERISTICS OF LIMESTONE IN SO_2 –RICH ATMOSPHERES: MECHANISMS AND KINETICS

MASTER'S THESIS

Dip. Eng. Özgür Bilinç YILMAZ

The Given Date of the Thesis: 08-06-1998

The Date of the Advocate: 29-06-1998

Supervisor : **Prof. Dr. Okan ADDEMİR**

The Other Referees : **Prof.Dr. Süheyla AYDIN**

Prof. Dr. Tuncer ERCİYES

JUNE 1998

İSTANBUL TEKNIK ÜNIVERSITESI ★ FEN BILIMLERI ENSTITÜSÜ

KİREÇTAŞININ YÜKSEK SO_2 İÇEREN ORTAMLARDA SULFATLANMA KARAKTERİSTİĞİ: MEKANİZMA VE KİNETİK

MASTER TEZİ

Met.Müh. Özgür Bilinç YILMAZ

Tezin Enstitüye Verildiği Tarih: 08-06-1998

Tezin Savunulduğu Tarih : 29-06-1998

Supervisor : Prof. Dr. Okan ADDEMİR
The Other Referees : Prof.Dr. Süheyla AYDIN
Prof. Dr. Tuncer ERCİYES

HAZİRAN 1998

PREFACE

This thesis has been financially supported by Outokumpu Research Center, Pori, Finland. The experimental part of the study has been carried out in the Laboratory of Materials Processing and Powder Metallurgy at Helsinki University of Technology, from September, 1997 to May, 1998.

I would like to express my deep gratitude to Docent Dr. Pekka Taskinen for providing me this challenging project. Also to Ms. Tuula Mäkinen for giving me the opportunity to be employed a summer trainee in Outokumpu Research Center.

Special thank is due to Docent Dr. Ari Jokilaakso for his advice and comments as a supervisor.

I would also like to thank Prof. Dr. Okan Addemir, Prof. Dr. Ercan Açma and Docent Dr. Onuralp Yücel for their great support during my education.

Also to Esa Peuraniemi for his great guidance, patience and driving.

To Juha Järvi and Tapio Ahokainen for their advice on the kinetic calculations of the study. To Dr. David Morton, for sharing my "alieness" and grammar corrections.

I would like to thank the personnel of the Laboratory of Materials Processing and Powder Metallurgy for creating the opportunities to carry out this study and for a most pleasant atmosphere.

Finally to my Family for helping me to become who I am.

May of 16th, 1998

Özgür Bilinc YILMAZ

TABLE OF CONTENTS

PREFACE ii

NOMENCLATURE v

LIST OF FIGURES vii

LIST OF TABLES ix

SUMMARY x

YHTEENVETO xi

ÖZET xii

CHAPTER 1. INTRODUCTION 1

CHAPTER 2. GENERAL VIEW OF LIMESTONE AND IT'S PROPERTIES 2

2.1. BASIC DEFINITIONS OF THE LIMESTONE 3

2.2. HISTORY 4

2.3. ORIGIN OF THE LIMESTONE 6

2.4. MINERALOGY 8

2.5. IMPURITIES 8

2.6. PHYSICAL PROPERTIES 9

CHAPTER 3. THE CONCEPT OF SLAG AND ITS FUNCTIONS IN METALLURGY 18

3.1. FUNCTIONS OF LIMESTONE IN THE SLAG STURCTURE 20

3.1.1. SLAG STRUCTURE 20

3.1.2. THE BASICITY OF SLAGS 23

CHAPTER 4. CONDITIONS IN THE OUTOKUMPU FLASH SMELTER REACTION SHAFT. 25

4.1. BASIC CHEMICAL REACTIONS IN THE REACTION SHAFT 26

CHAPTER 5. TEORETICAL SURVEY OF SULFATION CHARACTERICSTICS OF LIMESTONE 29

5.1. PHYSICAL AND CHEMICAL MECHANISIMS OF THE SULFATION PROCESS 30

5.1.1. CALCINATION OF LIMESTONE 32

5.1.2. SULFATION MECHANISIMS OF CALCINED LIMESTONE 34

5.1.3. GRAIN AND SHRINKING CORE MODELS FOR THE SULFATION OF LIMESTONE 40

CHAPTER 6. EXPERIMENTAL APPROACH TO SULFATION MECHANISMS AND KINETICS OF LIMESTONE AT HIGH TEMPERATURES IN RICH SO_2 ATMOSPHERES 43

6.1. EXPERIMENTAL PROCEDURE 44

6.1.1. MATERIALS 44

6.1.2. EXPERIMENTAL APPARATUS 47

6.1.3. ANALYTICAL METHODS 50

6.2. EXPERIMENTAL RESULTS AND DISCUSSIONS 51

6.3. REACTION KINETICS OF HIGH TEMPERATURE SULFATION OF LIMESTONE 63

CHAPTER 7. CONCLUSIONS AND RECOMENDATIONS 68

REFERENCES 71

CURRICULUM VITAE 74

NOMENCLATURE

δ = boundary layer (m)

ε = Porosity

τ = Tortuosity

ΔH = Heat of reaction (cal/g/mole)

A = Arrhenius number

$A_{reaction}$ = Reaction surface area

C_a = Concentration of a (g.mole/m^3)

$D_{a,b}$ = Molecular binary diffusivity of A and B (m^2/s)

D_r = Diameter of Reaction layer (m)

k_{ov} = Overall reaction rate (m/sec)

k_r = Chemical reaction rate parameter (m/s)

$k_{so2,b}$ = diffusion rate of SO_2 through to boundary layer (m/s)

M_A = molecular weight of A (g/mole)

n_a = Number of moles of species (M)

R = Universal gas constant (= 1,987 cal/g/mole/K)

Re = Reynolds number

r_i = Unreacted core radius (m)

r_p = Grain radius (m)

Sc = Schmidt number

Sh= Sherwood number

t = Time (sec)

T_g = Gas Temperature (K)

T_p = Particle Temperature (K)

V_a = Diffusion volumes of molecule a (L^3/M)

X_a = mole fraction of a in mixture

$X_{a,b}$ = Mole fraction of a in bulk fluid and at surface

LIST OF FIGURES

Figure 2-1. Unit Cellular Structure of Calcite. 12

Figure 2-2. Unit cellular Structure of Dolomite. 12

Figure 2-3. Mean Specific heats of calcite and dolomite at different temperature . 16

Figure 3-1. The structures of molten solutions of a metal oxide in silica. 22

Figure 3-2. The structure of (a) solid orthosilicate and (b) molten orthosilicate in which dissociation of the silica network is complete. Further additions of metal oxide would produce free oxygen ions 23

Figure 4-1. Outokumpu Flash Smelting Furnace 25

Figure 4-2. Suspension characteristics of the reaction shaft 27

Figure 5-1. Schematic diagram of the calcination model. 33

Figure 5-2. Phase Stability Diagram of Ca-S-O System. 38

Figure 6-1. SEM Images for Surface Characteristics of Limestone. 46

Figure 6-2. Schematic Diagram of the Experimental System. 49

Figure 6-3. Effect of the Bed Thickness on Sulfation Ratio in Atmosphere Type 1 (10% SO_2, 70% O_2, 20% N_2) at 1200°C. 53

Figure 6-4. Effect of Atmosphere Types on Particle Fractions at 1200°C. 54

Figure 6-5. Sulfation Ratio of limestone in Atmosphere Type 1. 56

Figure 6-6. Calcined and Slightly Sulfated Limestone Particle Fraction +53-75μm. Atmosphere Type 2 at 1200°C ~ 2 h 40 m 57

Figure 6-7. Effect of the Different Atmospheres on the Particle Fraction +212-300μm at 1200°C. 58

Figure 6-8. Partially Sulfated Limestones. 59

Figure 6-9. Particles which were etched by phenolphthalein solution. 61

Figure 6-10. Schematic Diagram of the Shrinking Core Model 64

Figure 6-11. Weight and temperature Changes by Time 65

Figure 6-12. Mass change per second by Temperature. 66

Figure 6-13. Cumulative Overall Reaction Rate of the Sulfation Process 67

Figure 7-1. Equilibrium Composition of $CaSO_4$ 69

LIST OF TABLES

Table 2-1. Refractive indices for the sodium D line at 18^{O}C 13

Table 2-2. Diffuse Reflecting Power 14

Table 2-3. Calcium Carbonate's Ratio Of Solubility At Various Temperatures 17

Table 6-1 Chemical Analyses of Limestone 45

Table 6-2 Particle Fractions and Surface Areas of the Limestone 45

Table 6-3 Atmosphere Types of the Experiments. 47

Table 6-4. Overalll Chemical and X-ray Analyses 62

SUMMARY

The aim of the this study was to determine sulfation characteristics of limestone in the flash smelting furnace reaction shaft. Reaction shaft has been simulated in a vertical tube furnace by combining TGA measurement equipment. TGA records have been corrected to $CaSO_4/CaO$ ratio according to results of the analyses.

Three different Types of atmospheres have been used for simulating different parts of the reaction shaft. Contents of the atmosphere were as following: :

Atmosphere Type 1: 10 % SO_2, 70 % O_2, 20 % N_2

Atmosphere Type 2: 30 % SO_2, 10 % O_2, 60 % N_2

Atmosphere Type 3: 50 % SO_2, 2 % O_2, 48 % N_2

Limestone has been classified to four different fractions and each fraction has been examined in three atmospheres. Particle fractions of limestone were: +53-75, +106-150, +212-300, +600-850 μm. Furnace temperature was 1200°C in the experiments.

Reacted samples have been analyzed by Chemical and X-ray methods for giving the idea of reaction products. SEM–EDS combination and light microscope have used to determine product layer of the samples.

Shrinking core model has been applied for kinetic calculations of the sulfation reactions. Effect of diffusion of reaction gases has been calculated as well as porosity and tortuosity ratio.

YHTEENVETO

Työn tarkoituksena oli selvittää kalkkikiven sulfatoitumisominaisuuksia liekki-sulatusuunin reaktiokuilussa. Kokeissa reaktiokuilua simuloitiin pystysuoralla putki-uunilla, johon oli yhdistetty TGA laitteisto. TGA mittaukset muutettiin $CaSO_4/CaO$ - suhteeksi analyysitulosten perusteella.

Kokeissa käytettiin kolmea erilaista kaasuatmosfääriä kuvaamaan reaktio-kuilun eri osien olosuhteita. Kaasuseosten koostumukset olivat:

Kaasuseos 1: 10 % SO_2, 70 % O_2, 20 % N_2

Kaasuseos 2: 30 % SO_2, 10 % O_2, 60 % N_2

Kaasuseos 3: 50 % SO_2, 2 % O_2, 48 % N_2

Kalkkikivi luokitettiin neljään raekokoluokkaan, kaikki fraktiot tutkittiin kolmella kaasuatmosfäärillä. Raekokoluokat olivat: +53-75 µm, +106-150 µm, +212-300 µm ja +600-850 µm. Uunin lämpötila oli 1200C kaikissa kokeissa.

Reagoineet näytteet analysoitiin kemiallisia- ja röntgenmenetelmiä käyttäen reaktiotuotteiden selvittämiseksi. SEM - EDS menetelmää ja valomikroskooppia käytettiin reaktiokerrosten tutkimiseen näytteistä. Sulfatointireaktioden kineettisissä laskuissa käytettiin kutistuvan ytimen mallia. Kaasujen diffuusion vaikutus reaktiohin laskettiin, samoin kuin huokoisuus- ja kiemurtelevuussuhteiden vaikutus.

KİREÇTAŞININ YÜKSEK SO_2 İÇEREN ORTAMLARDA SULFATLANMA KARAKTERİSTİĞİ: MEKANIZMA VE KİNETİK

ÖZET

Yüksek saflıkta metal üretimi, tüm üretim çemberinin, cevher hazırlama aşamasından yüzey temizleme işlemine kadar dikkatle kontrol edilmesini gerektirir. Pirometalurjik üretim yöntemlerinde ergitme ve rafinasyon işlemleri prosesin en önemli adımlarındandır. Cürufun ergime noktasını aşağıya çekecek, metalle çözünürlügü az ve aynı zamanda maliyet açısından düşük olacak flux seçimi, ergitme işlemlerinin kritik bir aşamasıdır.

$CaCO_3$ slag oluşumunu sağlayan, nötrleştirme işlemlerinde kullanılan ana bileşiklerden birisidir. Özellikle 1970'li yılların başlarında çevre güvenliği kanunlarında yapılan değişiklikler, üretim sonucu ortaya çıkan atık gazların daha sıkı denetlenmelerini zorulu kılmıştır. Atık gazlardaki SO_2'in giderilmesi, $CaCO_3$ vasıtası ile absorbe edilerek temiz ve kolay yoldan sağlanabilmektedir. Bu amaca yönelik olarak özellikle akışkan yatakta kömürün yakılması sonucu ortaya çıkan SO_2'in bağlanmasına yönelik olarak bir çok araştırma yapılmıştır. Ancak bu söz konusu durumda gazdaki SO_2 içeriği max. 3000 ppm (0.3% v/v) civarına ulaşmakta ve proses sıcaklığı 1100°C'yi geçmemektedir. Öte yandan özellikle flash ergitme yöntemi ile bakır, nikel veya kurşun üretim yöntemini düşündügümüzde SO_2 içerği 70 % v/v civarlarına ulaşabildiği gibi sıcaklıkta 1400°C'ye kadar yükselmektedir. Bu etmenler göz önünde tutularak konuya yeni bir bakış açısı kazandırma ihtiyacı üzerine bu çalışmaya karar verilmiştir.

Bu çalışmadaki genel amaç, $CaCO_3$'in flash ergitme yöntemlerindeki genel karakterini ortaya koymaktır. Bu amaca yönelik olarak yapılan bu calışma Outokumpu Araştırma Merkezi (ORC; Pori, Finlandiya) tarafından desteklenmiştir. Projenin deneysel kısmı Helsinki Teknoloji Üniversitesinde tamamlanmıştır.

Çalışmada 4 ayrı tane boyutu aralıgında (+53-75, 106-150, +212-300, +600-850 μm) $CaCO_3$ kullanılmış. Tüm boyut aralıkları ayrı ayrı, flash fırının karekteristik özelligini temsil eden üç değişik atmosferde incelenmiştir.

Atmosfer 1: 10 % SO_2, 70 % O_2, 20 % N_2

Atmosfer 2: 30 % SO_2, 10 % O_2, 60 % N_2

Atmosfer 3: 50 % SO_2, 2 % O_2, 48 % N_2

$CaCO_3$ deneylerde kullanılmadan önce kimyasal analizi ve yüzey alanı ölçümleri yapılmış, yüzey karakteri, Scanning Electron Microscope (SEM) vasıtası ile belirlenmiştir. Deneylerde kullanılan malzeme aynı zamanda Harjavalta (Finlandiya) Flash Fırını'nında flux malzemesi olarak kullanılmaktadır.

Deneyler bir düsey tüp fırında flash fırın reaksiyon shaftının özellikleri sağlanarak 1200°C'de gerçekleştirilmiştir. Deney süresince platin bir pota içerisinde bulunan numunenin agırlık değişimi Thermogravimetric Balance System'i (TGA) vasıtası ile devamlı olarak kayıt edilmiştir.

Numune fırına oda sıcaklığında yerleştirilmiş ve fırın atmosferi izole edilerek gazların fırına enjeksiyonuna başlanmıştır. Gazların enjeksiyonu 15 dk. süre ile oda sıcaklığında yapılmış böylece fırın içerisinde deney atmosferi her hangi bir reaksiyon gerçekleşmeden önce sağlanmıştır. Deney atmosferi sağlandıktan sonra fırın deney sıcaklıgına kadar ısıtılmıs ve reaksiyonların tamamlanmasına kadar bu sicaklıkta sabit olarak tutulmuştur. Reaksiyonlar tamamlandıktan sonra numune fırın içerisinde ve N_2 gazı atmosferi altında oda sıcaklığına kadar soğutulmuştur.

Reaksiyonlar sonucu olusan atık gazlar 90% oranında seyreltilmis NaOH içinde nötralize edlirek açık atmosfere bırakılmıştır. Oluşan nötralizasyon çözeltisine çevre kanunlarındaki gerekli bazıklık oranını sağlayacak ilaveler yapıldıktan sonra endüstriyel atık barajinda depolanmıştır.

Tüm deneyler sırasında numunenin öncelikle kalsinasyonunun tamamlandığı ve daha sonra sulfatlanma reaksiyonlarının başladıgı saptanmıştır. Bu nedenle hesaplamalarda $CaCO_3$ yerine CaO kullanılmasının daha uygun olacagına karar verilmiş ve hesaplamalar CaO üzerinden yapılmıştır.

Fırından alınan numune üç ayrı kısma ayrılarak analiz işlemleri için sınıflandırılmıştır. Genel olarak numuneler reaksiyon zonlarına göre üst, orta ve alt kısımlardan ayrı ayrı alınmış ve bir desikator içinde muhafaza edilmiştir.

Numunelerin, x-ışınları ve kimyasal analizleri Outokumpu araştırma merkezinde gerçekleştirilmiştir. Numuneler ayrıca SEM–EDS kombinasyonu kullanılarak analiz edilmiş ve reaksiyon ürünlerinin yüzey karekteristikleri belirlenmiştir. Bu amaca yönelik olarak, tane kesiti şeklinde numuneler hazırlanmış ve bu numunelerin yüzeyleri ince bir altın tabakası ile kaplanmıştır.

Değişik analiz teknikleri numunelere EDS vasıtasıyla uygulanmış ve numunenin içerdigi elementler belirlenmiştir. Bu amaçla x-ışınları analizlerinde $CaSO_4$'dan başka bir faz içermeyen (***Mg tüm analizlerde MgO formunda belirlenmiştir***) numunelerde nokta veya alan analiz yöntemi, kısmen reaksiyona

uğramış numunelerde ise element haritalama ve çizgi analiz yöntemleri kullanılmıştır.

SEM-EDS analizlerinin yanı sıra numuneler ışık mikroskobu ile incelenmiştir. Bu çalışmadaki amaç ise tam olarak sulfatlanması tamamlanmamış olan numunelerin reaksiyon ara yüzeylerinin görselleştirilmesidir. Bu amaca yönelik olarak tane kesiti numuneleri phenolphthalein çözeltisi ile dağlanmıştır. CaO bileşiğinin alkali karekterinden yararlanılarak yapılan bu calışmada, tanelerin yüzey kısımında oluşan asidik karekterli sülfat tabakasında bir değişiklik olmazken, merkezde bulunan CaO bölgesi renk degiştirerek beyazdan kırmızı renge dönmüştür.

Öncelikle, deneylerde kullanılacak malzemenin optimum miktarının belirlenmesine yönelik olarak deneylere başlanmıştır. Bu amaca yönelik olarak, +53-75 μm boyut aralığındaki malzeme çesitli miktarlarda platin pota içerisine yerleştirilerek sulfatlanma karekteri incelenmiştir. Bu amaçla yapılan deneylerde 1 g $CaCO_3$ pota içersinde 6 mm'lik bir kalınlık teşkil etmiş ve sonuçta 98 % oranında sulfatlanması sağlanmıştır. Bu adımdan sonra deneylerin geri kalan bölümünde 1 g baslangıç malzemesi ile devam edilmesine karar verilerek, diger tane boyutlarının değişik atmosferlerdeki davranışlarının incelenmesine başlanmıştır.

1 no.lu atmosferin oksidasyon karekteri nedeni ile reaksiyona tabii tutulan $CaCO_3$ >95 %'den fazla oranlarda sulfatlanmış ancak tane boyut aralığı +600-850 μm olan numune ise 80 % oranında sulfatlanabilmiştir.

2 ve 3 numaralı atmosferlerin indirgen karekterleri nedeni ile bir miktar sulfatlanma sağlandıktan sonra reaksiyonlar durmuştur. Bunun yanı sıra tane boyutunun etkiside özellikle 3 numaralı atmosferde daha belirgin olarak ortaya çıkmış ve değişik hipotezlerin ışıgı altında bu davranışlar analiz edilmiştir.

Sulfatlanma prosesi sırasında tanelerin sinterleşmesi gözlenmiştir. Özellikle numune yüzeyinde porositesi düşük, reaksiyon ürünleri tabakası nedeni ile oluşan difüzyon bariyerleri yüksek $CaSO_4/CaO$ oranlarının elde edilebilmesini engellemiştir.

Bu calışmada ayrıca $CaCO_3$'in reaksiyon kinetiğide incelenmiştir. Bu amaca yönelik olarak "Shrinking Core Model" uygulanmıştır. Model tane boyut aralıgı +53-75 μm olan ve 1 numaralı atmosferde reaksiyona tabii tutulan numune için tatbik edilmistir. Modelde yapılan bazı kabulleri şöyle sıralamak mümkündür:

i. Tanelerin ve fırının sıcaklığı aynı kabul edilmiştir.

ii. Numune öncelikle 100 % oranında kalsine edilmiştir. Sullfatlanma prosesinin baslangıç noktası olarak CaO baz alınmış ve kütle değişimleri aşağıdaki reaksiyona göre hesaplanmıştır.

$$CaO + SO_2 + 1/2O_2 = CaSO_4$$

iii. İlk iki dakika içerisinde 30 % üzerinde sulfatlanma gerçekleşmiştir. Bu sürenin kısalığı ve yerterli veri olmayışı baslangıçta kimyasal reaksiyon kontrollu olan bu aşamanın parametrelerinin saptanabilmesini olanaksız hale gertirmistir.

iv. Taneler küresel olarak kabul edilmis ve ortalama tane boyutu 64 μm olarak kullanılmıştır.

v. Taneler tabaklar halinde dizilmis kabul edilerek, hesaplamalar bir tabaka üzerinden yapılmıştır.

Kütle difüzyonu ile kontrol edilen aşama için yapılan hesaplamalarda parameterler, por yapısının ve SO_2'in reaksiyon ara tabakasından, reaksiyon yüzeyine difüzyonun toplam reaksiyon hızına etkisini inceleyecek sekilde tasarlanmıştır.

Por yapısının önemli ölçüde reaksiyon hızını kontrol ettiği saptandıktan sonra, diger bir adım olarakta porosite ve tortuosite etkisi üzerine yogunlaşılmış ve elde edilen sonuçlardan görüldügü üzere sistemde porların kilitlendiği saptanmıştır.

Benzer karakterde bir çalışmaya literatür arastırması sırasında rastlanmadığından kinetik hesaplamalardan ortaya çıkan sonuçların karşılastırmalı tartışması yapılamamıştır.

$CaCO_3$'in sulfatlanma karekteristiği termodinamik açıdan incelendiğinde ise sıcaklığın olumsuz bir etkisi oldugu görülmektedir. Gerek faz stabilite diagramlarından gerekse HSC programı yardımı hesaplanan denge diagramlarından görüldüğü üzere artan sıcaklıkla birlikte oluşan $CaSO_4$'in parçalanma eğilimi taşıdığı veya $CaSO_4$ yerine CaS'in oluşumunun popüler hale geldiği saptanmıştır. Özellikle redüktif atmosfer altında $CaSO_4$ bileşiğinin CaS ve CaO şeklinde parçalandığı kayıt edilmiştir.

Atmosfer 2 ve 3 altında yapılan deneylerden elde edilen sonuçlar, bu teorinin önem kazandığını göstermektedir. Bu deneyler sırasında reaksiyonlar sona erdikten sonra fırın sıcaklığının düşürülmesi üzerine yeniden sulfatlanma reaksiyonlarının başladığı görülmüştür.

Bu atmosferlerde yapılan deneyler sırasında N_2 gazı koruması altında fırının oda sıcaklığına sogutulma sürecinde reaksiyonlar tekrar başlamıştır. Bu fazladan sulfatlanma reaksiyonlarından korunulamadığı için analizlerde verilen değerler bu miktarlar üzerinden verilmiştir. Ancak dönüşüm oranı olarak kullanılan $CaSO_4/CaO$ oranı direkt olarak sistemden alındığı için bu oranlarda deney sıcaklığında reaksiyonların sona erdigi andaki degerler kullanılmıştır.

Bu çalışma sırasında gözlenmiştir ki, yüksek oranlarda SO_2 ile calışılan sistemlerde korozyon açısından sistem ve ekipmanlarının çok dikkatle seçilmesi gerekmektedir. Gaz kontrol sistemleri ve gaz akışını düzenleyen ekipmanlar her türlü nemden arındırılmalı, plastik malzeme kullanımından sakınılmalıdır. Metalik kısımların özellikle SO_2 ve bilesiklerine karşı resistan olanları seçilmelidir.

Gazların fırın içerisinde izolasyonları iyi sağlanmalı ve çevre güvenliği açısından gerekli önemler alınmalıdır.

Diğer önemle üzerinde durulması gereken bir husus ise özellikle CaO içeriği yüksek reaksiyon ürünlerinin depolanması ve analiz numunelerinin hazırlanmasıdır. Aşırı hidroskopik karekterli olan CaO desikator içerisinde saklanmalı ve tane kesiti numuneleri alkol-lubrikant karışımı ile önerilen en düşük sürelerde hazırlanmalıdır. Bu konuda dikkat edilmesi gereken ikinci bir nokta ise Ca–bileşiklerinin çok sert bir yapı göstermeleri nedeni ile tane kesiti numunelerinin hazırlanma zorluğudur. Zımpara ve parlatma malzemeleri imkanlar ölçüsünde dikkatle ve önemle seçilmelidir.

Konunun flash fırındaki önemi açısından, $CaCO_3$'in bakır konsantreleri ile karıştırılarak benzer şartlar altında incelenmesinin ve ara reaksiyon mekanizmalarının belirlenmesi gerekliliği gözlenmiştir.

Alternatif olarak öncelikle sulfatlanma reaksiyolarını tamamlayan numunelerin indirgen atmosfer altındaki reaksiyon mekanizmalarının incelenmesinin gerekli olacağı gözlenmiştir.

CHAPTER 1

INTRODUCTION

The production of high purity and quality metals takes into consideration the whole production chain from ores to metals. In pyrometallurgical treatments smelting process is one of the most important step. Choosing the right fluxing materials for the lowest melting point is critical for production of clean slags and metals. The flux material also has to provide the lowest solubility of the valuable metals in the slag regardless of the concentration of impurities.

Limestone is the main compound for both formation of slag and for neutralization processes required to ensure environmental safety. Hence, it is impossible to produce many metals and alloys without using limestone. Understanding its behavior for conditions of production increases the opportunity for controlling process parameters.

In order to provide additional information that can be used to benefit operation of process, this study is based on the reaction mechanisms and kinetics of the limestone in high SO_2 contents at 1200°C. Experiments were carried out in a vertical tube furnace by combining thermogravimetric analyzing method. The reacted samples were analyzed using different analytic techniques.

In the following chapters, limestone is discussed from its basic characteristics to its behavior in the sulfation reactions.

CHAPTER 2

GENERAL VIEW OF LIMESTONE AND IT'S PROPERTIES

There are a few absolutely indispensable forms of matter, like air and water, that are generally taken for granted by humankind but without which life simply would cease. Similarly on this, there are other almost equally basic and essential materials without which life would be, at the very least, completely barren (and possibly not sustainable) and modern commerce and industry could not exist. Among these ancient, prosaic, unglamorous, and low-cost materials are lime and limestone. Literally any object that exists in people's home, their office (or virtually any manufactured product) has required lime or limestone in some phase of its manufacture, directly or indirectly, either as a prime or incidental processing material [1].

Limestone's abundance is evidenced by the fact that an estimated 3.5 to 4% of the minerals in the earth's crust contain calcium and 2% contains magnesium. Of all elements, calcium ranks fifth in abundance, only exceeded by oxygen, silicon, aluminum, and iron. Of course, as with most elements, there are strata of lime stone laminated between layers of shale and sandstone that are so deep in the earth's crust as to be inaccessible. There are great many different forms and types of limestone, varying in color, chemical composition, mineralogy, crystallinity, texture, and hardness. There are also other important calcium and magnesium bearing rocks and minerals like gypsum, phosphate rock, serpentine, and fluorspar, that should not be confused with limestone since they

are not carbonate rocks, an essential characteristics of limestone, but none of these natural resources are as basic [1].

2.1. BASIC DESCRIPTIONS OF LIMESTONE

Lime and limestone are much abused terms. Often users, and even some sellers, will refer to some form of limestone as lime and less often vice versa. Limestone is a general term embracing carbonate rocks or fossils; it is composed primarily of calcium carbonate or combinations of calcium and magnesium carbonate with varying amounts of impurities, the most common of which are silica and alumina. In contrast, lime, which is invariably derived from limestone, is always a calcined or burned form of limestone, popularly known as *"quicklime"* or *"hydrated lime"*. The calcination process expels the carbon dioxide from the stone, forming calcium oxide (quicklime), and when water is added, calcium hydroxide (hydrated or slaked lime) is created. While all three of these products have some similarities, the correct connotation of these terms is important since there are many pronounced differences [1].

An analogy to the close relationship of limestone and lime would be sulfur and sulfuric acid. The former are the native ores, which in spite of processing are still used in their original chemical composition. The limestone group consists of the most basic alkalies; sulfur is at the other end of the pH scale- the most basic acid. The uses of these two sets of materials are at the same time totally diverse, complementary, and often interchangeable. There are a sufficient number of overlapping uses for lime to regard limestone as its principal competition. However, from a tonnage standpoint the main competitors for limestone would be other aggregates, like sand and gravel, granite, basalt, etc [1].

2.2. HISTORY

Lime and limestone are prehistoric and among the oldest materials used by mankind. The use of limestone is an outgrowth of the Stone Age, in which primitive man utilized limestone and other forms of rock to confine fires, construct stone shelters, and make crude tools and weapons. It is conjectured that lime was discovered later in the same age. One intriguing theory on its discovery is that primitive man probably found his slabs of limestone, used for fireplaces, disintegrating into a white paste-like putty following a hard rain. The stone had been calcined by the heat from his fires, and the resulting quicklime was simply hydrated by the rain water. The pyramids built by the Egyptians between 4000 and 2000 BC, however, are the first recorded use for limestone and employ huge nummulitic limestone blocks and lime along with alabaster (gypsum) for mortar and plaster. Marble statuary and luxurious wall construction was initiated shortly after this period. Although lime's use originated for construction, it was employed by the Greek and early Roman empires also as a chemical reagent. Xenophon in 350 BC records how a ship carrying a cargo of linen and lime "for its bleaching" was wrecked near Marseilles. Cato mentioned the burning of the lime in kilns in 184 BC. The medical use of saturated solutions of lime water was cited by the Roman, Dioscorides, in 75 AD. The first great highway builders, the Romans, used both limestone and lime extensively. There was even some application and recognition of the virtues of agricultural liming at the time of Christ[1].

One of the early forms of chemical warfare was the reported gruesome practice of the English in throwing quicklime in the faces of the French, during a war in 1217 AD. Shakespeare and earlier English writers, like Layamon, frequently mentioned lime in their writings. European alchemists in the Middle Ages are known to have causticized the potassium carbonate present in wood ashes with lime to produce a crude form of lye as a base for soapmaking[1].

The first sound technical explanation of lime calcination, including its expulsion of CO_2 gas, was by the British chemist, Joseph Black, in the eighteenth century. The French scientist Lavoisier, a few years later confirmed and extended Black's theory. Other renowned French scientists–Vicat, Debray, and Le Châtelier–in the nineteenth century are credited with measuring most of the earliest fundamental data, including the dissociation temperature and pressure incident to calcination as well as evaluating structural limes and mortars for construction [1].

Strangely, many of the ancient civilizations appear independently to have discovered lime and perfected their own uses of it. Some civilizations, for example the Greeks undoubtedly learned from each other. But who at that time educated such isolated civilizations as the Incas, Mayas, Chinese, and Mogul Indians? Their ancient applications of lime have been repeatedly confirmed by archaeologists through the artifacts they have unearthed. Somehow they all "stumbled" upon its uses by primitive ingenuity or happenstance. Fragmentary decipherings of their scarce records reveal some barbarous methods of making lime mortar, such as slaking quicklime in barley water, mixing blood from animals into the lime and sand, etc. Yet some of their old edifices stood for two to three thousand years, dissheveled from the erosion of time but still intact and often structurally sound. Restoration societies have rescued many of these old structures from desuetude and have remortared their eroded joints with modern cementing materials. Ironically often these modern scientifically prepared mortars disintegrate in five to twenty years, requiring repeated expensive maintenance, in contrast to the thousands of years that the ancients' bizarre mortars have endured. Possibly modern civilization has not advanced in some respects as much as we think [1].

2.3. ORIGIN OF THE LIMESTONE

In defining and describing limestone and its properties more emphasis will be placed on its physical and chemical than on its geological characteristics. This most important and abundant of all sedimentary rocks that is employed commercially is usually of organic origin fossiliferous, marine sedimentation in oceans and fresh bodies of water, consisting of shells and skeletons of plants and animals, were gradually accumulated through deposition, layer upon layer to form in some instances massive beds of limestone. Some of this sediment was deposited by natural chemical reactions, namely, the infinitesimal dissolution of these calcium carbonate fossils through the solvent action of carbon dioxide, forming calcium bicarbonate, which was subsequently reprecipitated in carbonate form. Sometimes this precipitation is indirect through the intermediary of plant and animal organisms. Direct precipitation of the carbonate through a saturated solution is caused by either an increase in temperature, which reduces the solubility of the calcium carbonate, or through evaporation. Originally fossils were formed by gradual assimilation of carbonate as a bicarbonate from seawater, inducing a very slow but inexorible build-up of the shell or skeletal structure. On the demise of the organism its shell of almost pure calcium carbonate remains as a nucleus to perpetuate the above phenomena. It is a true reversible reaction with dissolution and precipitation in approximate equilibrium [1].

Huge coral reefs are gradually accumulated in this manner over thousands of years, and in the millions of years of geologic ages that have reshaped the geography of the world, they have formed mountains in the interior of continents. Many mountains in Europe and North America are coralline in origin. Pressure and heat have supplemented chemical precipitation in consolidating the minute carbonate particles into these imposing compact masses [1].

In a similar manner inland streams and rivers are carriers of soluble calcium bicarbonate through the leaching effect of rainwater percolation through soils in watersheds and the gradual dissolution of carbonate rocks as the streams

cascade over them. The co-reactant, carbon dioxide, must be present to effect this phenomena. Most soils contain at least traces of calcium and magnesium; some are highly calcareous. Such soluble calcium is the most common type of hardness mineral that exists in varying amounts in fresh-water bodies [1].

The texture and crystalline form of limestone depends on the size and shape of the calcareous particles or grains that are deposited. Usually this deposition is contaminated with varying amounts of impurities, like silica, that through time becomes an intimate part of the stone, seemingly cemented to the carbonate particles. Generally the purest limestone formations occur more often in the thickest masses or beds of up to several hundred meters thick. However, frequently these thick beds will contain strata of relatively impure stone. Contamination of the stone usually occurs at the commencement of deposition, but in some instances impurities can be absorbed through pores and interstices during deposition. These impurities occur both vertically and laterally in the bed, but usually a change in purity is much more gradual laterally than vertically [1].

The calcareous sediment may remain relatively soft, like chalk or marl, or it may be metamorphosed through high temperature and fused into a highly crystalline form, such as marble. Examples of limestone that are not of organic origin would be stalactites and stalagmites in caves and some oolitic limestone, travertine, and calcareous tufa. However, the presence of fossils in varying degrees is apparent in most commercial limestone, and this enables the geologist to determine from which geologic age it was derived. Often the prehistoric fossils are found intact in the stone in an almost perfect state of preservation [1].

The other common constituent of limestone, magnesium carbonate, is also formed in a related manner, but it is thought that much of it was created by chemical displacement of calcium with magnesium from magnesium salts that abound in seawater. Decomposition of serpentine (hydrous magnesium silicate) would be another possible origin [1].

2.4. MINERALOGY

All geological authorities are agreement that limestone may be composed of four minerals, exclusive of impurities, having the following physical characteristics:

Calcite. $CaCO_3$; rhombohedral; molecular weight–100.1; specific gravity–2.72; molecular volume– 36.8; hardness–3; may be colorless, but often variously tinted by impurities[1].

Aragonite. $CaCO_3$; orthorhombic; specific gravity–2.94; molecular volume–34; hardness–3.5 to 4; usually white but often tinted by impurities[1].

Dolomite. $CaMg(CO_3)_2$; rhombohedral; molecular weight–184.4; specific gravity–2.83; molecular volume–65.2; hardness–3.5 to 4; usually colorless, but often tinted[1].

Magnesite. $MgCO_3$; rhombohedral; molecular weight–84.3; specific gravity–3; molecular volume–28.1; hardness–3.5 to 4.5; white, tan or brown[1].

2.5. IMPURITIES

There are two classifications of impurities: **1.** homogenous, in which the impurities in the form of clay, silt, and sand (or other forms of silica, like quartz), contaminate the stone when it is first deposited and in which the impurities are well dispersed throughout the formation and **2.** heterogeneous, in which the impurities collect only in the crevices or between the strata or as siliceous pieces or nodules of sand, chert, or flint loosely embedded in the limestone. This is the source of silica and alumina, the major impurities. A minor source of silica is derived from feldspar, mica, talc, and serpentine [1].

Iron is the third major impurity and can be homogeneously disseminated after the limestone has started to form by chemical displacement of the calcium, producing iron carbonates. This frequently occurs in oolitic limestone. Another source of iron would be oxide, distributed heterogeneously from such materials as pyrite, limonite, magnetite, and hematite, but only rarely in the latter two [1].

Phosphorus and ***sulfur*** usually occur but generally in small quantities. Chemical displacement of the carbonate radical by oxy-acid radicals of these two elements is a homogeneous source of impurity. Additionally, phosphorus is also derived from certain fossiliferous skeletons (invertebrates) forming the nucleus of calcareous deposits. Pyrite is another source of sulfur [1].

The remaining impurities are so minute that they could be considered as *trace elements* in the relatively pure stones. These might be manganese, copper, titanium, sodium and potassium (as oxides), fluorine, arsenic, strontium, etc...[1].

2.6. PHYSICAL PROPERTIES

Depending upon the type of carbonate rock, most of the physical properties will vary, often considerably. Complete values for all varieties of limestone are not available, but in the compilation of the following properties the magnitude of these values is at least revealed, and often very precise measurements are presented[1].

Color. Pure forms of the minerals, calcite and magnesite, are white, often with an opaque cast, but most conventional limestone, even the purest types, are grey or tan. The grays, caused by carbonaceous impurities, often become dark grey, even approaching black. The presence of iron influences the tannish color and other related hues of buff, red, and brown. There are dolomites with a pinkish surface cast, although generally dolomite crystals are pearly in color and in granular form have a dull, earthy luster. The presence of other mineral impurities,

like pyrite, marcasite, and siderite, may alter the surface color on oxidation through weathering [1].

Of course, with the more unconventional species of limestone, like marble or travertine, there are a myriad of scintillating colors of diverse mottled and variegated effects that are famed for their exquisite beauty; others are milky white [1].

Texture. X-ray diffraction has revealed that all limestone is crystalline. However, the size, uniformity, and arrangement of its crystalline structure or mineral grains vary greatly, forming stone of divergent density and hardness [1].

Porosity. There is considerable variance in the degree of porosity, which is determined as the percentage of pore space (or absorption value) in the stone's total volume. Total porosity ranges generally between 0.3 and 12% of the stone. The former represents the so-called compact or dense kinds and the latter the softer, more porous species. Certain dense, fine-grained stone can be cut by machines precisely and polished to simulate marble in smoothness. Most of the porous stone contains water in varying amounts. Porosity of marble is the lowest– as low as 0.1 % [1].

Crystal Structure. X-ray diffraction reveals that all calcitic and dolomitic limestones are crystallized in the rhombohedral system. In contrast, aragonitic $CaCO_3$ is orthorhombic. The molecular structure of calcite and dolomite are depicted in Figs.2.1 and 2.2 respectively, demonstrating that slight differences occur in the dimensions and angles of their unit cells. Inclusion of the smaller Mg atom in the dolomite lattice reduces the cell edge from 6.36 Å for calcite to 6.02 Å and the cell angle 47°6′ to 46°6′. Pure $MgCO_3$ (magnesite) has still smaller edge dimension of 5.61 Å but a larger angle of 48°12′ [1].

Bulk Density. Because of the difference in porosity the bulk density of limestone ranges between about 2.0 $g.cm^{-2}$ to 2.8 $g.cm^{-2}$. Stone that contains moisture weighs slightly more than its dry counterpart. The denser, more impervious types weigh over 2.4 $g.cm^{-2}$. On an average, the bulk density of dolomite is slightly greater than high calcium by about 2.5% [1].

Specific Gravity. Pure calcite is considered to have a specific gravity of 2.7 at 20°C. The rare mineral, aragonite, is heavier 2.93. However, most commercial limestone has a range in values 2.65 to 2.75 for high calcium and 2.75 to 2.90 for dolomitic. Values for magnesian are intermediate but closer to high calcium in value. Chalk is much less-between 1.4 and 2.0 [1].

Hardness. Pure calcite is standardized on Moh's scale at 3.0, whereas aragonite is harder, ranging between 3.5 and 4.0. Commercial limestone varies considerably 2 to 4. Dolomite is generally harder than high calcium stone, but its crystal is relatively brittle and tends to break with an uneven to conchoidal fracture. Most limestone is soft enough to be readily scratched with a knife [1].

Strength. There is also a wide variance in the strength of limestones. Generally marble and travertine are among the highest values; chalk and marl are among the lowest. Some of the cherty, impure stones have very high strengths. Compressive or crushing strengths range between 84.37 and 1996.72 $kg.cm^{-2}$. Shear strength values typically range between 42.18 and 210.9 $kg.cm^{-2}$; however, some marble has been measured as high as 456.9 $kg.cm^{-2}$. Tensile strength has been reported between 24.61 to 63.28 $kg.cm^{-2}$ [1].

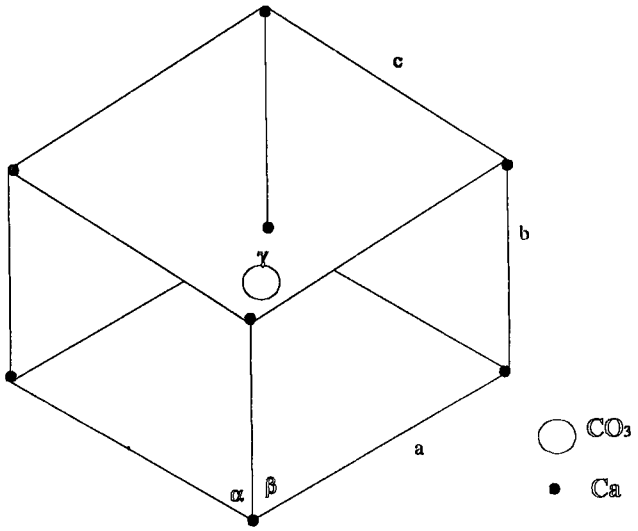

a=b=c=6.36.Å α=β=γ=46°6′

Figure 2-1. Unit Cellular Structure of Calcite.

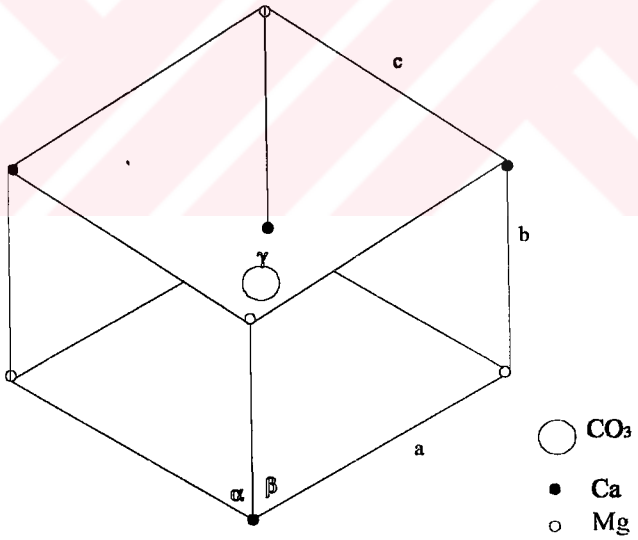

a=b=c= 6.02 Å α=β=γ= 47°7′

Figure 2-2. Unit cellular Structure of Dolomite.

Modules of Rigidity. As the reciprocal to the modulus of elasticity, reported values for this characteristic extending from 105460.44 to 358565.49 $kg.cm^{-2}$ for eleven different high calcium and dolomitic limestones [1].

Coefficient and Expansion. From 0 to 300°C the expansion of limestone is negligible but does increase with temperature. Between 20 and 50°C the coefficient of expansion of oolitic limestone was been measured at 0.000005 /°C [1].

Young's Modulus. Values range between 224982.26 to 864775.58 $kg.cm^{-2}$ [1].

Poisson's ratio. Values range between 0.07 to 0.35 [1].

Refractive index. Calcitic or aragonitic crystals possess much greater optical or refractive properties than dolomite. Increasing iron content causes the refractive index of the latter to heighten. Calcitic crystals exhibit double refraction; in contrast, dolomite produces negative double refraction [1].

Table 2-1. Refractive indices for the sodium D line at 18°C [1].

Calcite	Aragonite
μω 1.6584	μα 1.5300
με 1.4864	μβ 1.6812
	μγ 1.6857

Luminescence. Both calcite and dolomite have limited luminescent qualities. Fragments of dolomite transmit light poorly or not at all, depending on the impurities present. Both pure forms of dolomite and calcite are luminescent when exposed to cobalt–60γ–radiation; calcite when exposed to short-wave radiation. Some varieties of calcite will phosphoresce after exposure to ultraviolet light and can be made to fluoresce and appear purple. In contrast, pure dolomite appears colorless under ultraviolet light except for small bands of purple caused by an excess of $CaCO_3$ in the dolomitic lattice [1].

Diffuse Reflecting Power. This is ratio of total luminous flux reflected to that received, measured for the various regions of the spectrum. The wavelengths are those of maximum energy [1].

Table 2-2. Diffuse Reflecting Power [1].

	Reflecting Power %					
Material	0.54	0.60	0.95	4.4	8.8	24.0
$MgCO_3$	–	85.2	89.4	10.8	4.1	8.8
Limestone*	–	42.9	–	20.3	5.0	–
$CaCO_3$ Marble†	–	53.5	–	6.4	5.1	–

* Indiana, dense, fine-grained.
† White color, ground, unpolished.

Velocity of Sound. The velocity of sound through marble has been calculated to be 3810 $m.sec^{-1}$ [1].

Thermal Conductivity. Values for white marble in $cal.cm^{-3}.sec^{-1}.{}^{o}C^{-1}$. are given as follows: 50-100 = 0.00614; 100-150 = 0.00524; 150-200 = 0.00415. No values are found for limestone or dolomite, but they are conjectured to be slightly lower [1].

Heat Capacity. Values in $cal.gram^{-1}$ are cited for: limestone 0.24 at 58°C, marble 0.19 at 0°C, marble 0.24 at 200°C [1].

Specific Heat. At a temperature of 37.78°C and stated in $cal.gram^{-1}$, the specific heats for high calcium and dolomitic limestones are 0.114 and 0.120 respectively. The specific heats increase as the temperature rises, as depicted in Fig.1-3, but a specific heat value of 0.01 has been measured for calcite at 250.8°C. Specific heats of pure calcite have been measured and are similar to Figure .2.3. More limited values given for aragonite appear to be very similar to calcite [1].

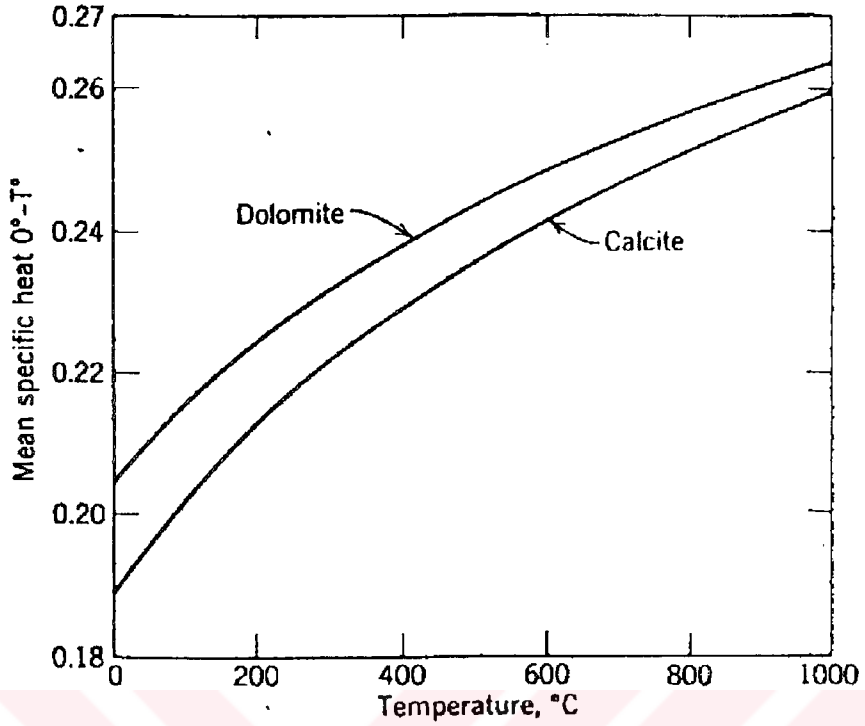

Figure 2-3. Mean Specific heats of calcite and dolomite at different temperature [1].

Melting Point. Since all limestone is transformed into oxides before melting or fusion can occur, no values are given here. The melting point of quicklime is 2570°C [1].

Heat of Formation. In the formation of calcite by $CaO + CO_2 = CaCO_3$, the heat of this reaction is 42,600 cal.mole^{-1} at 25°C. The only value for magnesite that appears plausible is 28,900 cal.mole^{-1}. Dolomite is intermediate between these two values [1].

Electrical Resistivity. In ohms.cm^{-1} values are reported as follows: limestone 10^5; marble 10^{10} [1].

Dielectric Constant. Values are given: limestone 8 to 12; dolomite 7.3; marble 8.3 [1] .

Solubility. In pure distilled water that is devoid of dissolved CO_2 and in a CO_2–free atmosphere, limestone is virtually insoluble, but with increasing partial pressures of CO_2 solubility increase steadily to the point where it might be characterized as slightly soluble.

The ratio of solubility for calcium carbonate (at one atmosphere) have been calculated at various temperatures. These calculations are shown in Table 2.3 which indicate that solubility steadily decreases as the temperature is raised above 0°C.

Table 2-3. Calcium Carbonate's Ratio Of Solubility At Various Temperatures [1].

Temperature	0°	10°	20°	25°	30°	50°
Ratio	1.8	1.4	1.1	1.0	0.9	0.6

CHAPTER 3

THE CONCEPT OF SLAG AND ITS FUNCTIONS IN METALLURGY

Slags are alloys of vàrious oxides, which may form chemical compounds, solid and liquid solutions and eutectic mixtures. A principal function of metallurgical slags is to remove gangue from the furnace and thus to separate it from other molten product (metal, matte, etc...) [2].

Besides their principal function, metallurgical slags fulfill a number of other no less important functions [2]. These functions are summarized as follows:

1.Slags are the site of chemical reactions of utmost importance in many extractive metallurgy processes. For example, in reduction smelting of lead silicates, dissolved in slag, is reducted by gases and solid carbon (coke). The losses of metals in slag depend substantially on the degree of completeness of these reactions[2].

2.Droplets of metal or matte settle in the slag, thus ensuring separation of the metallic part of the burden from the gangue. One of the principal forms of metal losses in slags is mechanical loss due to poor settling [2].

3.Slag composition generally determines the maximum or minimum temperature which can be obtained in shaft-type furnaces [2].

4.Slags interact with the metallic bath in smelting and refining of metals and alloys, thus governing the refining efficiency and the concentration of impurities in the metal produced [2].

5.Sometimes slags are not wastes, but the main product containing the base metal, which is then separated from the impurities concentrated in other products [2].

6.Slags serve as binders in sintering of ores and concentrates. For example, when lead concentrates or fine copper ores are sintered in preparation for shaft-furnace smelting, the low-melting slags cement grains of the burden on cooling of the sinter [2].

7.A coat of the slag, however thin, protects the metal against saturation by furnace gases or oxidation [2].

8.Slags may serve as resistor elements in metallurgical processes involving the application of electric power [2].

These numerous functions of slags predetermine the wide scope of requirements to physical and chemical properties of slags in various cases. In some processes low-melting slags are preferred, in others, by contrast, high narrow-range melting point is required, in blast furnace operation or in the production of ferroalloys. In some cases, slags should be acidic whilst in others basic slags are more appropriate [2].

The presence of dissolved sulfides, chlorides and other salts, and off-gases (SO_2 in particular), greatly affects the metallurgical properties of slags (in the first place, their melting points and viscosities) [3].

A drop in the viscosity and the lowering of the melting point of a slag due to a dissolution of gases is similar to a decrease in the freezing point of water observable on solution of gases in it (SO_2, CO_2, air, etc.). In addition, many gases are mineralizers of slag promoting their crystallization (or melting) at a lower temperature. A similar decrease in the viscosity of a melt on dissolution of gases may be observed in eruptive rock; in some cases the presence of gases lower the melting point of eruptive rock and slags by 100-150°C [3].

3.1. FUNCTIONS OF LIMESTONE IN THE SLAG STURCTURE

3.1.1. Slag Structure

Extraction slags are formed from the oxides among the gangue minerals which can be made fluid at a reasonable temperature by the addition of a suitable flux–usually another oxide and often in the form of a low grade ore of the metal being extracted, an ore with a different type of gangue. The slag should ideally have low solubility for oxide of the metal being smelted, to ensure a high yield. For siliceous gangue, CaO and FeO are common fluxes, while limy gangue might be fluxed with silica sand [4].

Refining slags are specially prepared to be capable of absorbing, usually as oxides, impurities from the metal, and may incorporate chemical reagents for converting these impurities into soluble or volatile forms [4].

At higher temperatures anions become smaller and cations more numerous. An ultimate structure consisting of an equal number of SiO_2^{4-} and Si^{4+} ions can be envisaged but would require a very high temperature indeed. The

presence of very large anionic units is reflected in the very high viscosity of silica because the anions are not easily broken up by mechanical forces [4].

Basic oxides dissociate when dissolved in molten silica, e.g.

$$CaO = Ca^{2+} + O^{2-} \quad (3.1)$$

and in the presence of Si^{4+} ions,

$$Si^{4+} + 4O^{2-} = SiO_4^{4-}. \quad (3.2)$$

This would be accompanied by some further dissociation of large anions to restore the equilibrium implicit in equations;

$$4.5SiO_2 = Si_3O_9^{6-} + 1.5Si^{4+} \quad (3.3)$$

$$10.5SiO_2 = [Si_9O_{21}]^{6-} + 1.5\ Si^{4+} \quad (3.4)$$

So that continued additions of CaO would ultimately reduce all the complex ions to SiO_4^{4-} tetrahedra at the composition corresponding to the orthosilicate, i.e. $2CaO.SiO_2$. Other basic oxides would behave in a similar manner (see Figures 3-1, 3-2) [4].

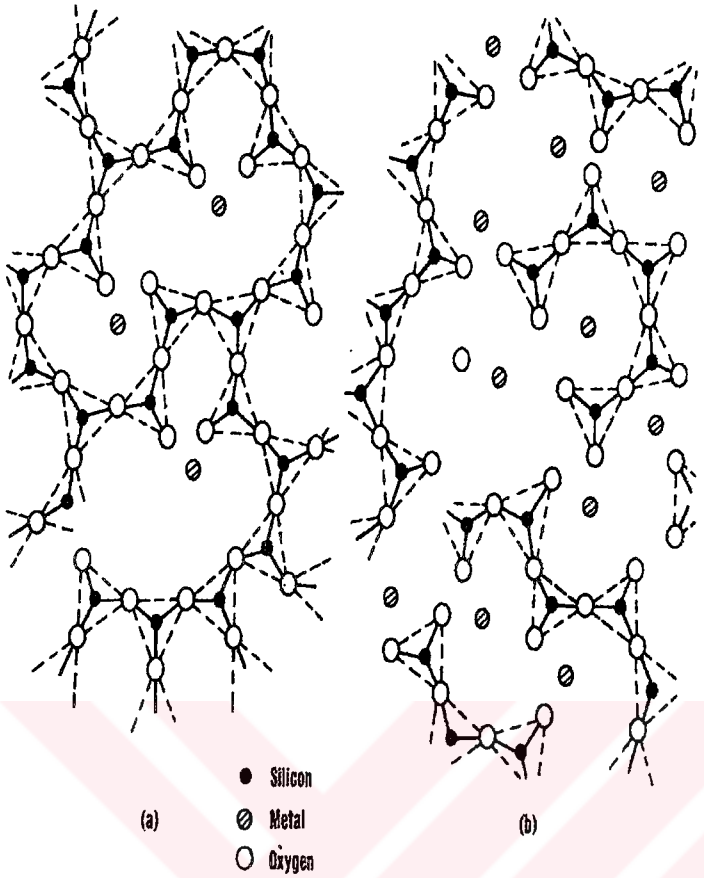

Figure 3-1. The structures of molten solutions of a metal oxide in silica, the proportion of metal oxide being higher in (b) than in (a) [4].

Further additions of CaO beyond the orthosilicate proportions are presumed to dissociate into equal numbers of Ca^{2+} and O^{2-} ions. The whole arrangement must maintain short-range electrical neutrality and high entropy so that even in very short distances the composition is very close to the average for the melt. There is no suggestion of the formation of molecules [4].

Other slag constituents behave either like silica or lime. Fe_2O_3 may form FeO_3^{3-} ions. The common basic oxides (like FeO, MnO, MgO) dissociate to produce S^{2-} ions which can replace free O^{2-} ions but sulfur cannot take the place of the oxygen atoms in the anionic groups [4].

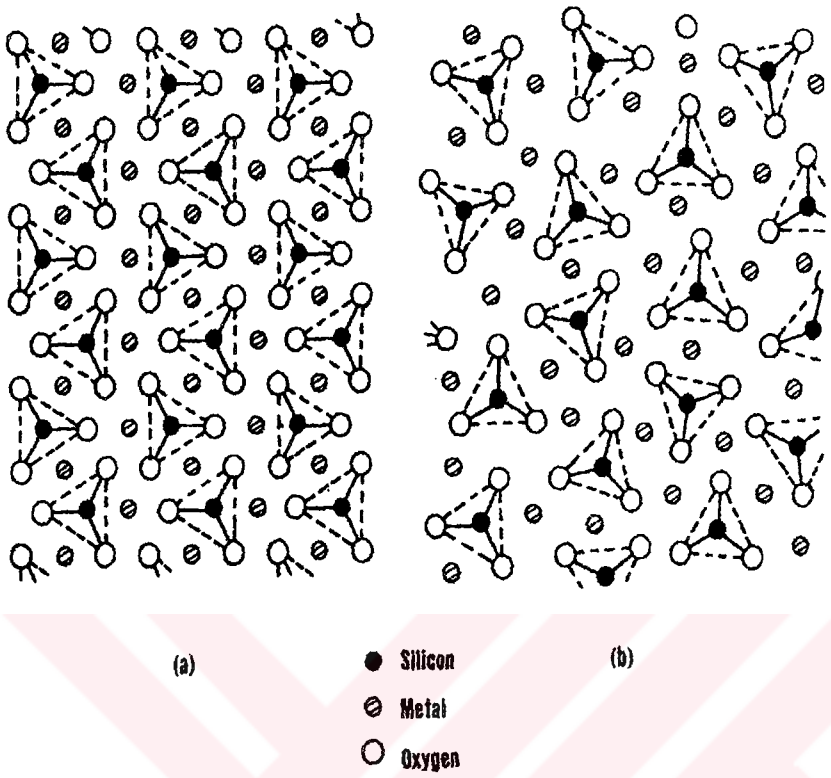

Figure 3-2. The structure of (a) solid orthosilicate and (b) molten orthosilicate in which dissociation of the silica network is complete. Further additions of metal oxide would produce free oxygen ions[4].

3.1.2. The Basicity of Slags

In terms of the ionic theory a "basic" slag is one in which there are free O^{2-} ions and an "acid" slag one in which there are no free O^{2-} ions but which has a high capacity for incorporating them into their more complex structures. Thus acidic slags attack refractories made from basic oxides and vice versa.

Quantitatively the degree of basicity has been expressed in several ways. The simplest expression is the CaO/SiO_2 ratio (by weight). And the ratio $(CaO + MgO)/(SiO_2 + Al_2O_3)$ might appear to be better but there is some doubt as to the

"equality" of CaO and MgO and that of SiO_2 and Al_2O_3. It is sometimes reduced to $(CaO + 2/3\ MgO)/SiO_2$ on the grounds that MgO is a weaker base than CaO and Al_2O_3 plays part as an acid (or receiver of O^{2-} ions). The exact role of each constituent may depend upon the kind of slag and it is often stated that Al_2O_3, being an amphoteric oxide, behaves as an acid only in very basic slags. Fe_2O_3 is similar, being mentioned as an acid oxide only in connection with very basic oxidizing slags. The ratios mentioned above are all in weight per cent [4].

CHAPTER 4

CONDITIONS IN THE OUTOKUMPU FLASH SMELTER REACTION SHAFT.

Flash smelting technology can be divided into the following classifications: Outokumpu flash smelting, Inco flash smelting, and cyclone smelting[5]. The Outokumpu flash smelting furnace (Figure 4-1) has been developed for production of copper, nickel and lead from their sulfuric concentrates[6]. To date, there are 38 flash smelting licenses sold for copper, nickel and sulfur production world-wide[6].

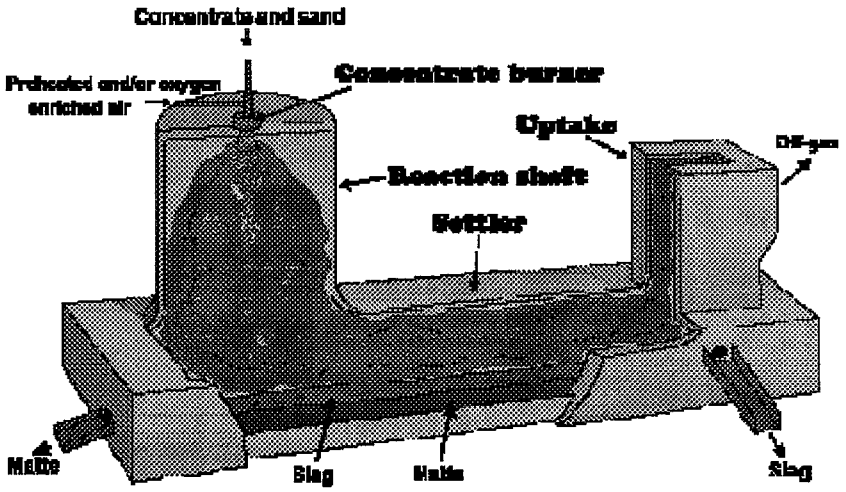

Figure 4-1. Outokumpu Flash Smelter Furnace [6].

Copper flash smelting consists of blowing fine, dried copper sulfide concentrate and silica flux with air, oxygen-enriched air or oxygen blast into a hot (~1500 K) hearth-type furnace. Entry of these materials into the hot furnace causes the sulfide minerals (e.g. $CuFeS_2$) of the concentrate to react rapidly with the O_2 of the blast[7].

4.1. BASIC CHEMICAL REACTIONS IN THE REACTION SHAFT

Reactions in the flash furnace reaction shaft may be represented by equations of the type:

$$2CuFeS_2 + \frac{13}{4}O_2 \longrightarrow \underset{matte}{(Cu_2S \cdot \frac{1}{2}FeS)} + \frac{3}{2}FeO + \frac{5}{2}SO_2 \qquad \Delta H^0_{298} = -450\ MJ/kgmol\ CuFeS_2 \qquad (4.1)$$

$$FeS_2 + \frac{5}{2}O_2 \longrightarrow FeO + 2SO_2 \qquad \Delta H^0_{298} = -700\ MJ/kgmol\ FeS_2 \qquad (4.2)$$

$$2FeO + SiO_2 \longrightarrow \underset{slag}{2FeO \cdot SiO_2} \qquad \Delta H^0_{298} = -20\ MJ/kgmol\ FeO \qquad (4.3)$$

Reactions (4.1) and (4.2) are strongly exothermic. They provide most or all of the energy for heating, melting and superheating the furnace products. In fact, when industrial oxygen or highly oxygen enriched air is used to provide the O_2 for reactions (4.1) and (4.2), little or no fossil fuel needs to be combusted in the furnace [7].

The first stage is ignition of the concentrates, which takes place at 300-400°C. Due to effective mixing of concentrate and oxygen enriched air combustion takes place close to the concentrate burner exit without the need for a supporting flame. When ignited the temperature of the particle rises above that of the surrounding gas [8].

The maximum temperature and SO_2 content are reached at about the same time in 1-2 seconds in the normal suspension, which is produced initially by a distributor. Suspension characteristics are given in Figure 4-2 [8].

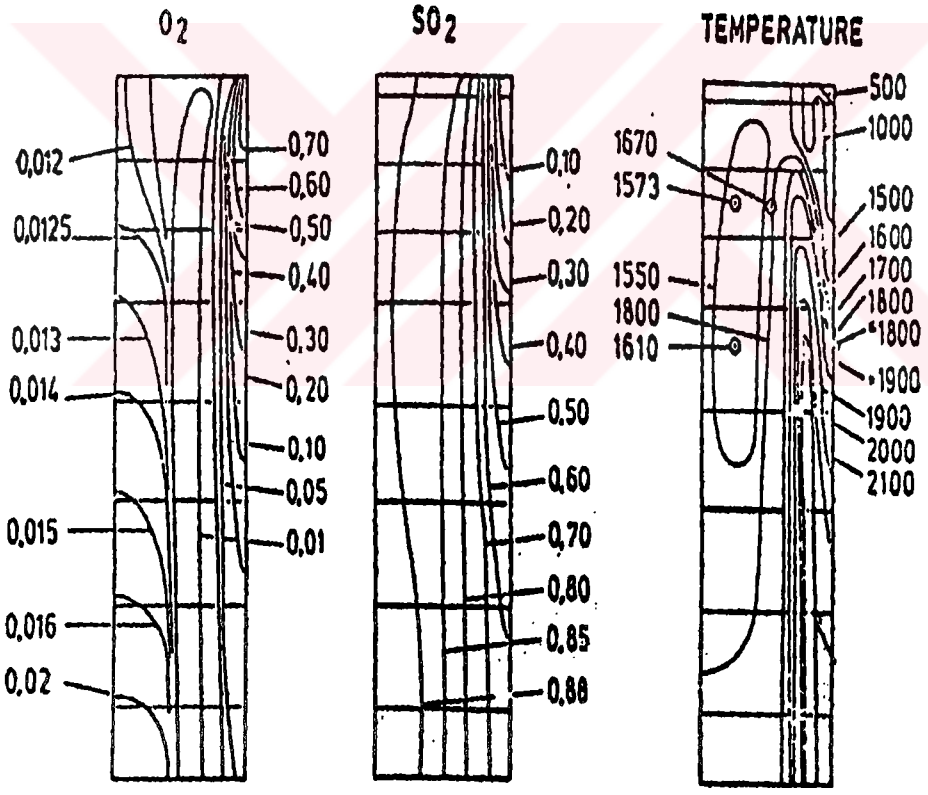

Figure 4-2. Suspension characteristics of the reaction shaft[8].

Since copper smelting in a flash furnace is based on partial oxidation of concentrate particles, a knowledge of the extent of oxidation of the particles falling through the reaction shaft can assist in understanding the reaction mechanism between the particles and gas composition in the reaction shaft [5].

CHAPTER 5

TEORETICAL SURVEY OF LIMESTONE SULFATION CHARACTERISTICS

Considering the conditions of flash smelting furnace in the terms of atmosphere and temperature characteristics, examining sulfation behavior of the limestone according of these conditions is becoming more important.

In this stage, different theories of particle and pore behavior and also thermodynamic and kinetic results on the reaction mechanisms from literature have been checked to suggest an understanding of the behavior in new conditions.

There are two different models which are used to explain characteristics of limestone during sulfation process according to particle behavior. These models can be named as grain model and shrinking core model. These theories consider the particle behavior rather than other effects.

Besides the effect of particle behavior, there were several effects on the ultimate sulfation ratios. These variables can be listed as effects of $[SO_2]$ and $[O_2]$, temperature and thickness of the limestone bed in the crucible. Consequences of these will be discussed in this and following chapters.

5.1. PHYSICAL AND CHEMICAL MECHANISIMS OF THE SULFATION PROCESS

Mechanism of absorption of SO_2 by $CaCO_3$ is not completely understood, primarily because of the inter-reaction between physical and chemical processes occurring within the particle. The structure of limestone (i.e. the pore and grain sizes) has fundamental importance when considering the progress of the reaction since diffusional limitations to the reaction rate eventually dictate the degree of sulfation of a particular stone [9].

Reaction between sulfur dioxide and limestone under oxidizing conditions can be described as at least two consecutive reaction steps, calcination and sulfation:

$$CaCO_{3(s)} \rightarrow CaO_{(s)} + CO_{2(g)} \qquad (5.1)$$

$$CaO_{(s)} + SO_{2(g)} + \tfrac{1}{2}\, O_{2(g)} \rightarrow CaSO_{4(s)} \qquad (5.2)$$

Under low oxygen pressures previously formed calcium sulfate may be decomposed to form calcium oxide and gaseous components [10].

One of the most interesting features of the sulfation process is the effect of temperature on the ultimate degree of conversion. The amount of SO_2 absorbed by limestone particle (at atmospheric pressure) appears to increase as the temperature is raised up to around 820-860°C. Beyond this temperature the SO_2 absorbed starts to decrease. This observation has been the subject of considerable speculation and several hypotheses have been proposed to explain it. It is

generally agreed that the origins of this phenomenon are chemical in nature, since the physical structure of the stone does not appear to affect materially the location of the optimum temperature. The main area of uncertainty lies in the identities of both the intermediate species formed in the absorption and of the two, or more, competing routes by which they are produced and reacted. The reaction may be visualized as occurring through one of the following processes[9]:

(a) Calcination of limestone

$$CaCO_{3(s)} \rightarrow CaO_{(s)} + CO_{2(g)} \quad (5.1)$$

(b) Initial oxidation of SO_2 to SO_3

$$SO_{2(g)} + 0.5O_{2(g)} = SO_{3(g)} \quad (5.3)$$

$$CaO_{(s)} + SO_{3(g)} \rightarrow CaSO_{4(s)} \quad (5.4)$$

(c) Formation of $CaSO_3$

$$CaO_{(s)} + SO_{2(g)} = CaSO_{3(g)} \quad (5.5)$$

$$CaSO_{3(s)} + 0.5\ O_{2(g)} = CaSO_{4(s)} \quad (5.6)$$

(d) Formation of sulfide / sulfate mixtures

$$4CaSO_{3(s)} \rightarrow 3CaSO_{4(s)} + CaS_{(s)} \quad (5.8)$$

$$CaS_{(s)} + 2O_{2(g)} \rightarrow CaSO_{4(s)} \quad (5.9)$$

To describe adequately the reactions between the gaseous SO_2 and O_2 with the porous solid CaO (which is produced by the calcination of limestone) the following issues require consideration:

(i) A systematic basis on which to select compounds for enhancing the reactivity of limestones.

(ii) Whether increased reactivity or conversion results from promoting the oxidation of SO_2 to SO_3 and thereby facilitating sulfation via reaction 5.4.

(iii) Whether the decrease in retention of SO_2 by limestones and dolomites observed in fluidised-bed coal combustors at temperatures above 1123 K is due to change in mechanism [11].

5.1.1. Calcination of Limestone

Calcination of a limestone particle involves several steps, each of which is potentially rate-controlling. They are: (1) heat transfer from the external surface to the reaction interface, (2) thermal decomposition of $CaCO_3$ at the reaction interface; and (3) mass transfer of CO_2 from the reaction interface to the bulk gas (Figure 5-1). For small limestone particles in the size range 1-90 μm and gas temperatures between 500-1000°C, Borgwardt [12] suggested that the calcination process was under chemical kinetic control and that the calcination rate was proportional to the BET surface area. Since limestones are not fully crystalline and contain varying porosity, the BET surface area is a measure of the total surface area, including the surface area contained in accessible pores. Under such conditions, calcination occurs over the total surface area, thereby displaying volumetric characteristics [13].

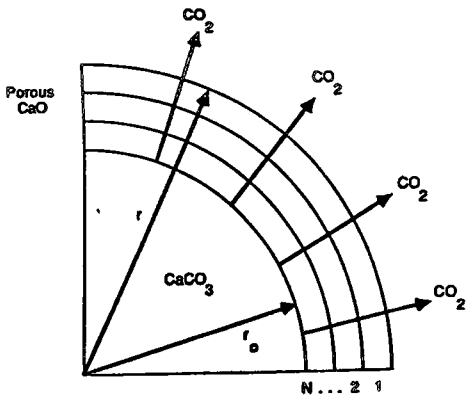

Figure 5-1. Schematic diagram of the calcination model.

The calcination process is described by a shrinking core model for a spherical particle. For massive samples of $CaCO_3$, heat transfer may limit decomposition rates, but for small, dispersed particles rates of heat and mass transfer are not rate limiting. For this reason, the particle is assumed to be isothermal and CO_2 concentration gradient exists across the CaO layer. The calcination process occurs in steps leading to a layered CaO zone (Fig. 5.1). The most recently formed layer of CaO has the highest surface area. The rate of surface area loss is a function of temperature, surface area and CO_2 concentration [14].

Several investigators [13-14], examined the effects of CO_2 pressure on decomposition kinetics. However, no one has developed an expression which is capable of explaining all of the data [14]. There is considerable experimental difficulty associated with precise determination of the calcination mechanism. For small limestone particles, the calcination interface is not easy to locate. Internal temperature gradients are difficult to measure, as is the local CO_2 partial pressure. For these reasons, most models of the calcination of small dispersed

particles assume that the particle surface temperature is equal to the bulk gas temperature, and that no internal temperature gradients exist [13].

The diffusion of gaseous CO_2 in porous lime was studied by Campbell [15] who showed the process is controlled by Knudsen diffusion. Knudsen diffusion is the controlling transport mechanism for CO_2 in porous lime; but, for moderately sintered CaO in which pore diameters are larger, ordinary diffusion becomes more important [14].

5.1.2 Sulfation Mechanisims of Calcined Limestone

The processes for sulfation of limestone or lime has been studied at lower temperatures (900-1000°C) for the lower sulfur dioxide contents (max. 3000 ppm = 0.3 v/v) [9-17]. On the other hand, when tonnage of oxygen is used in the flash smelting process, SO_2 concentration can be as high as 75% v/v and temperatures can reach as high as 1400°C [16]. According to their results, the following theory can be generalized for lower temperatures (<1100°C)

It was mentioned [9-17] that the sulfation reaction is very rapid in its initial stage. As the reaction time continues, however, the rate of reaction decreases rapidly. Previous investigators have observed that the rate of reaction can decrease with increasing time of reaction of CaO to SO_2. In their experiments reaction times were only of the order of seconds or minutes, in practice much longer reaction times are of interest [17]. After about 10-11 minutes of reaction about 31% of the total amount of calcium oxide in the particles was converted to sulfate with rather slow conversion for the temperatures close to 1258 K. Under comparable circumstances estimated initial rate differences of the sulfation can be as much as ten times bigger for different authors [9-17].

Overall reaction of limestone sulfation can be written as

$$CaCO_{3(s)} + SO_{2(g)} + 0.5O_{2(g)} = CaSO_{4(s)} + CO_{2(g)} \quad (5.10)$$

This heterogeneous reaction of solid calcium carbonate with gaseous sulfur dioxide and oxygen, can be accompanied by or involve the prior calcination of calcium carbonate.

$$CaCO_3 \rightarrow CaO + CO_2 \quad (5.1)$$

Reaction 5.1 is usually fast at high temperature and the reported results suggest that the overall reaction 5.10 may proceed to some extent by reaction 5.1 followed by reaction 5.2 [17].

$$CaO_{(s)} + SO_{2(g)} + \tfrac{1}{2}\, O_{2(g)} \rightarrow CaSO_{4(s)} \quad (5.2)$$

Limitations on the rate and extent of sulfation occur because $CaSO_4$ possesses a molar volume considerably larger than either the oxide or the parent carbonate (52 $cm^3.mole^{-1}$ compared with 17 $cm^3.mole^{-1}$ and 37 $cm^3.mole^{-1}$ respectively) and hence absorption of SO_2 inevitably introduces restrictions on diffusivities within the particle which eventually halt the reaction. The pore and grain structure produced during the calcination of the limestone is a key parameter

determining the utilization efficiency of the limestone, varying the calcination conditions before sulfation alters the ultimate degree of reaction attained by the stone. An extensive pore structure develops during calcination of limestone. However, the formation of calcium sulfate is accompanied by a net decrease in porosity. Sulfation causes large decreases in porosity, with porosities lower than original limestone. This is believed to be due to a combination of pore and grain size variation which leads to a greater amount of penetration of SO_2 into the interior of the particle before pore blocking occurs. The inertness of MgO component prevents a complete blockage of the pores and permits SO_2 and O_2 diffusion even at high sulfur loadings [9,17].

Previous workers [9-17] attempted to isolate the chemical influence in the sulfation process by measuring the absorption of SO_2 in different concentrations of O_2, and it was concluded that oxidation of SO_2 to SO_3 occurs before reaction with the calcium-containing interior of the particle as an intermediate. The formation of sulfate occurs at a rate dependent on the rate of SO_3 diffusion into the grains composing the particle. The concentration of SO_3 being determined by the diffusion of SO_2 and O_2 through the pores in addition to the kinetic parameters for oxidation. Barriers to diffusion are set-up by $CaSO_4$ production at rates dependent on the local $[SO_3]$ and hence variations in ultimate fractional conversion for a limestone reacted under different conditions may be related to changes in the SO_3 generation profile. Some limestones reacted to different extents when the oxygen concentration in the surrounding gases was varied: increasing the $[O_2]$ tended to provide lower conversions. This may be interpreted as being caused by changes in the location and speed of erection of the diffusional barriers to reaction, which induces variations in the distribution of sulfur throughout the stone. A high $[O_2]$ infers a high $[SO_3]$ at the edge of particle, which in turn causes a more rapid pore-plugging and a quicker cessation of the absorption. Increases in temperature have been observed to cause a shift in the sulfur distribution towards the outer edge of the stone presumably due to the faster kinetics of oxidation of SO_2 and hence a more rapid plugging of the pores by the $CaSO_4$ product [9].

Below 800°C the sulfur capture process is inhabited due to slow or incomplete calcination. A number of explanations have been put forward to explain the marked drop in sulfur capture performance at temperatures above 850°C. Several explanations are concerned with the porous structure of lime; they propose that a higher temperature results in an internal structure which is less suited to sulfur capture [9-23].

Literature data [22-23] of the thermodynamic stabilities of calcium-sulfur compounds suggest there is competition between sulfur capture under oxidizing conditions and release of sulfur under reducing conditions. Under oxidizing conditions $CaSO_4$ is stable, whereas CaS is stable under reducing conditions. There is an intermediate region where CaO is stable. The size of this region increases rapidly with temperature increase. The phase stability diagram can be seen in Figure 5.2. An increased reduction rate will produce active lime and increase the gross sulfur capture rate. The reduction of sulfate compounds are not "seen" as long as the net sulfur capture rate, (i.e. gross sulfur capture less reduction), is not markedly affected. A decrease in the net sulfur capture rate is furthermore concealed by the long residence time of the limestone particles. This permits complete sulfation even at a low net rate [22-23].

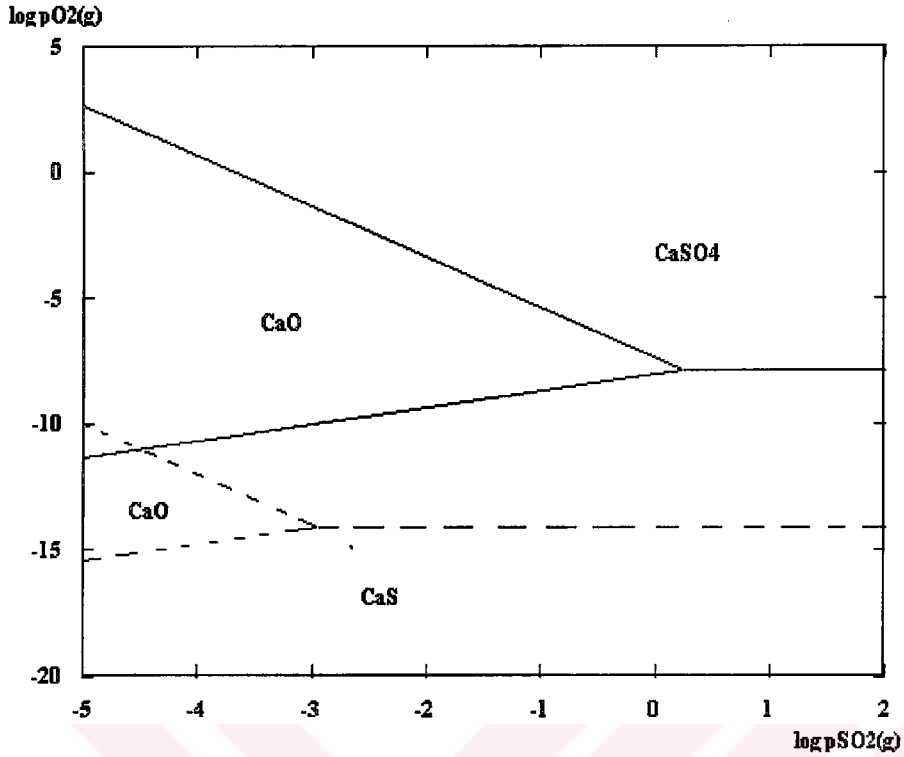

Figure 5-2. Phase Stability Diagram of Ca-S-O System [22].

"--------" Indicates Stability Areas at 800°C and "———" Indicates Stability Areas at 1200°C [24].

The reaction rates for both the release and the capture of SO_2 increase with temperature. Two factors, however, greatly promote the release rate as the temperature is increased: i. The shift in equilibrium pressure of SO_2 over $CaSO_4$ under intermediate conditions increases rapidly with temperature (Figure. 5-2), and ii. The increasingly reducing nature of the conditions in the particle phase caused by the combustion of volatiles and by increased char gasification and combustion rate [22-23].

The proposed competition between capture and release implies that at a 'given temperature and with stationary conditions' a balance in the amount of $CaSO_4$ and CaO arises. A temperature increase shifts the balance since the

desorption rate increases faster with temperature than does the absorption rate. This is observed as an increase in the SO_2 emission which subsequently decreases as a new balance is approached. If the amounts of $CaSO_4$ and CaO in the bed are large this new balance is approached slowly and the SO_2 emission will appear as a direct function of temperature [22-23].

The dependence of the sulfur capture behavior on temperature can be predicted from the assumption of a reductive decomposition of $CaSO_4$ under the conditions in the particle phase. The SO_2 capture rate decreases to zero when the temperature increases above 900°C, then increases again if the temperature is held constant. This behavior strongly indicates a desorption of SO_2 for the following reasons:

i. If the temperature dependence were explained solely by the arrest of the sulfur capture under reducing conditions, a level of zero would not be expected since some of the sorbent particles are in oxidizing regions.

ii. If the decrease in sulfur capture at higher temperatures is related to impairment of pore structure the following behavior would be expected: at a high temperature, a large amount of the reactive CaO would become impaired and accordingly the sulfur capture at a given temperature should be lower following a temperature decrease compared with that following temperature increase.

The effect of high volatile content would be to create more strongly reducing conditions in the particle phase. Thus higher volatile content would be expected to increase the rate of reduction of $CaSO_4$ [22-23].

5.1.3. Grain and Shrinking Core Models for The Sulfation of Limestone

Various models can be divided into three main groups (a) grain models, (b) pore models, and (c) network models. Within each group there are a number of modified models. In short, the grain model considers the solid particle to consist of small grains, the pore model considers the solid material to have a pore system and the network model is an inverted pore model, i.e. the solid material is assumed to consist of cylindrical rods with random intersections. All three concepts can take into account the structural changes that occur in the course of the reaction. The grain model and the pore models are the most commonly used [18].

Changing grain size model for gas-solid reactions has shown that a linear relationship exists between porosity and conversion not only in the average sense but also at each local radial position within a reacting pellet. According to previous studies [19-21] a critical value for initial porosity is established which determines whether complete conversion is possible. They analytically calculate a critical time, the pore plugging time, for which the pore at the pellet surface is blocked if the initial porosity is not larger than the critical value. The basic concept is that the porosity at the reacting pellet surface may become zero, which will then prohibit further reaction [19-21].

When the solid product is non-porous and forms a dense layer around the reactant solid, the transport of the gases across the product layer occurs by solid-state diffusion. The following assumptions have been used to describe solid-state diffusion and reaction of SO_2 within a porous spherical particle of limestone made up of a large number of uniform grains [19]:

1. Mass transfer to the external surface of the particle does not effect the rate of reaction.

2. The temperature is uniform in the whole system.

3. The grains are small enough so that variations in gas concentration on their surface can be neglected.

4.The reaction between the gas and the grains is of first order with respect to sulfur dioxide and proceeds by the unreacted shrinking core mechanism.

5.The reaction is taking place in the presence of excess of oxygen and is irreversible.

6.The pseudo-steady-state approximation is accurate enough for system.

Besides these assumptions, if particle shrinkage occurs during the decomposition, less volume is available for subsequent reaction. In large particles, internal concentration gradients cause calcium sulfate to form preferentially in pores near the surface, which then close or "plug". Further reaction is very slow and involves solid-state diffusion through this outer shell. In smaller particles, the sulfation occurs more uniformly throughout the particle. In this case, the rate of sulfation is controlled at the internal oxide grain level, usually by solid-state diffusion through the growing product layer of calcium sulfate. When the latter mechanism prevails, the rate is strongly affected by the diameter of the oxide grains and therefore by the internal specific surface area. Without particle expansion, the final conversion is limited by the porosity of the oxide particles [20].

The alternative shrinking model for non-catalytic gas-solid reactions finds many applications and for relatively coarse pellets or particles may indeed be the better practical approach for interpretation of experimental observations and for subsequent process design calculations involving multi-particle macro systems. It is assumed that reaction only proceeds at the interface between an inner unreacted

core and the outer reacted shell and reaction is referred to as being topochemical. When the unreacted core is dense this mechanism is predominant because the reacting gas cannot penetrate into the unreacted core. In general, if the reaction zone is narrow in comparison, with diameter of the solid pellet undergoing reaction then the shrinking core model may be acceptable [21].

CHAPTER 6

EXPERIMENTAL APPROACH TO SULFATION MECHANISMS AND KINETICS OF LIMESTONE AT HIGH TEMPERATURES IN RICH SO_2 ATMOSPHERES

Limestone is an important flux material for flash smelting process. Complete understanding of its behavior would support better control of the process. Considering the flash smelting complexity, knowledge of sulfation mechanisms and kinetics of limestone would help further studies of the more complex reactions.

Reactions of the limestone and SO_2 have been studied extensively with fluidised bed coal combustors. Changes in the environmental regulations at beginning of the 70's made this subject more popular due to the absorption of SO_2 cheaply and effectively. On the other hand, comparing conditions of coal combustors to flash smelting, lower temperatures and SO_2 contents make the current study necessary.

In this study, reaction shaft of the flash smelting furnace was simulated using a vertical tube furnace. Three different characteristic gas compositions of flash smelting have been examined at 1200°C. In addition to gas compositions experiments have been planned to demonstrate the effect of particle fractions and thickness of the limestone in the sample holder. The limestone used in the

experiments was provided by Outokumpu Research Center and is the same material that is used in the flash smelter.

At thermogravimetric balance system (TGA) was used for recording data during the experiments. Recorded TGA measurements have been used for further kinetic formulations. In addition to chemical and x-ray analyzing methods, SEM-EDS were also used to determine the surface characteristics of both raw materials and products. Boundary layers of the reacted particles were visualized by EDS analyzing methods and also using light microscope with an indicator.

Experimental part of the study has been carried out at the Helsinki University of Technology, Laboratory of Material Science and Powder Metallurgy, in Espoo, Finland. Chemical, x-ray, BET analyses were completed at the Outokumpu Research Center in Pori, Finland.

6.1 EXPERIMENTAL PROCEDURE

6.1.1. Materials

Limestone was provided by Outokumpu Research Center and is the same material used at flash smelter. A chemical analysis provided by the research center is shown as Table 6-1.

Table 6-1 Chemical Analyses of Limestone

Mineral	Weight (%)
$CaCO_3$	91.250
$MgCO_3$	2.150
SiO_2	6.6

Material was also classified according to particle size. Surface area of the each fraction was determined using liquid nitrogen and BET. Particle size classifications and BET measurements are given in the Table 6-2.

Table 6-2 Particle Fractions and Surface Areas of the Limestone

Particle Fraction No	Particle Size (μm)	BET surface Area (m^2/g)
Fraction 1	+53-75	1.92
Fraction 2	+106-150	1.43
Fraction 3	+212-300	1.65
Fraction 4	+600-850	1.58

Scanning Electron Microscope was used to determine surface characteristics of the raw materials as seen in Figure 6-1.

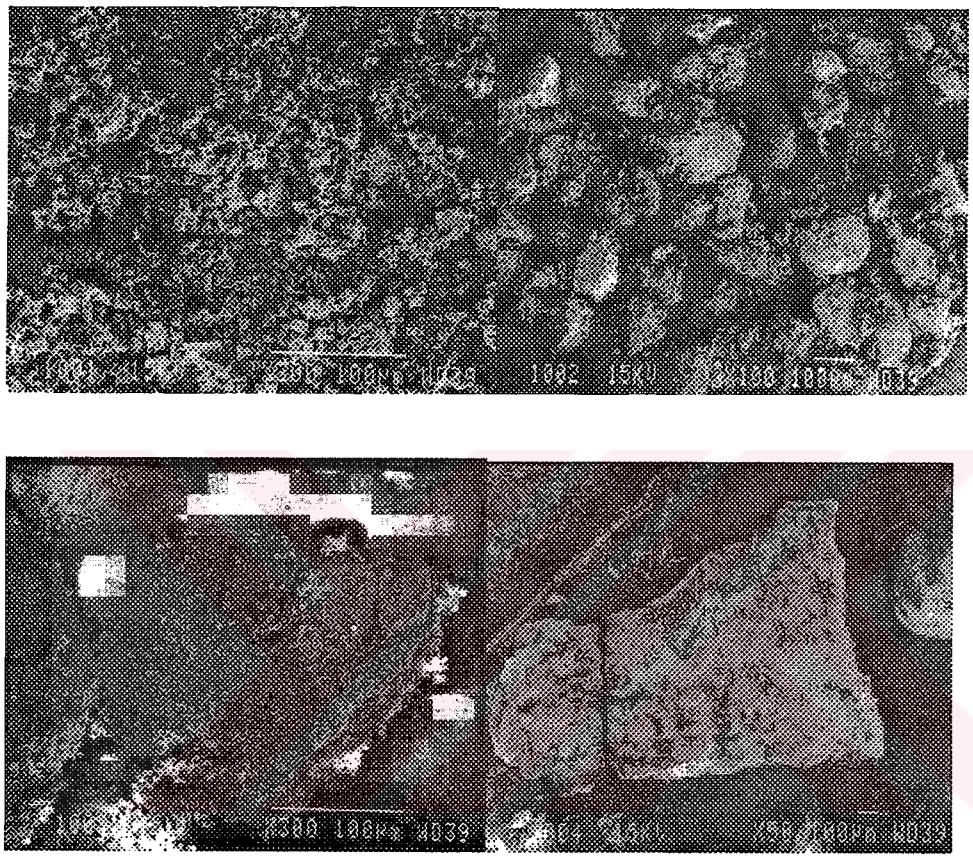

Figure 6-1. SEM Images for Surface Characteristics of Limestone. Each Picture Represents Fractions 1,2,3,4 Consequently.

Technically pure SO_2, O_2, and N_2 gases were mixed before being injected to the furnace. Moisture of the gas mixture was taken away by silica-gel bed. Three different types of atmosphere were chosen according to flash smelter reaction shaft characteristics. Atmosphere types of the experiments are given in the Table 6-3.

Table 6-3 Atmosphere Types of the Experiments.

Atmosphere Type	$SO_{2(g)}$ (% v/v)	$O_{2(g)}$ (% v/v)	$N_{2(g)}$ (% v/v)
Atmosphere Type 1	10	70	20
Atmosphere Type 2	30	10	60
Atmosphere Type 3	50	2	48

6.1.2. Experimental Apparatus

In the experiments, a vertical tube furnace (GWB made ROS 4/50 model) was used to simulate the reaction shaft of the flash smelter (Figure 6-2). Furnace temperature was controlled using two Pt-Pt(Rh10) S-type thermocouples. One thermocouple was used to stabilize the temperature of the furnace via a Eurotherm 818S model temperature controller. The other thermocouple was placed beside the sample holder to determine the correct sample temperature. The second thermocouple was connected to Graptec made Servocorder SR-6211 printer and Temperature calculations were performed using a HP 34401, a bench top model, math processor multimeter.

A thermogravimetric balance system (TGA) was used to determine sulfation degree according to the weight change of the samples. Weight change was measured using a Mettler, AT-261 Delta model balance and data was recorded via a Mettler GA-37 model digital-analog converter and printed for later examination.

To independently establish constant flow of each gas, a system of regulator valves was employed. Once gases passed through each valves they mixed together and passed through silica-gel tubes before being entering the furnace at a bottom injection point. Alumina nozzles were used to insure even gas distribution into the furnace. Nozzles and one of the thermocouple were sealed by a water cooled brass shield. Gas flow was calculated to be laminar in the furnace to avoid shaking of the sample holder and effecting the TGA measurements. Injection of reaction gas was started before heating the furnace so that precise atmosphere was attained before any reactions were taken place.

The reacted gas exits from a nozzle which is placed to the top of the furnace. Up-take gas was first washed-out in 10% NaOH solution to neutralize SO_2 according to Reaction 6.1. After neutralization, the gas passed into the open atmosphere.

$$2NaOH_{(l)} + 2SO_{2(g)} + 1.5O_{2(g)} = 2NaSO_{4(l)} + H_2O_{(l)} \qquad (6.1)$$

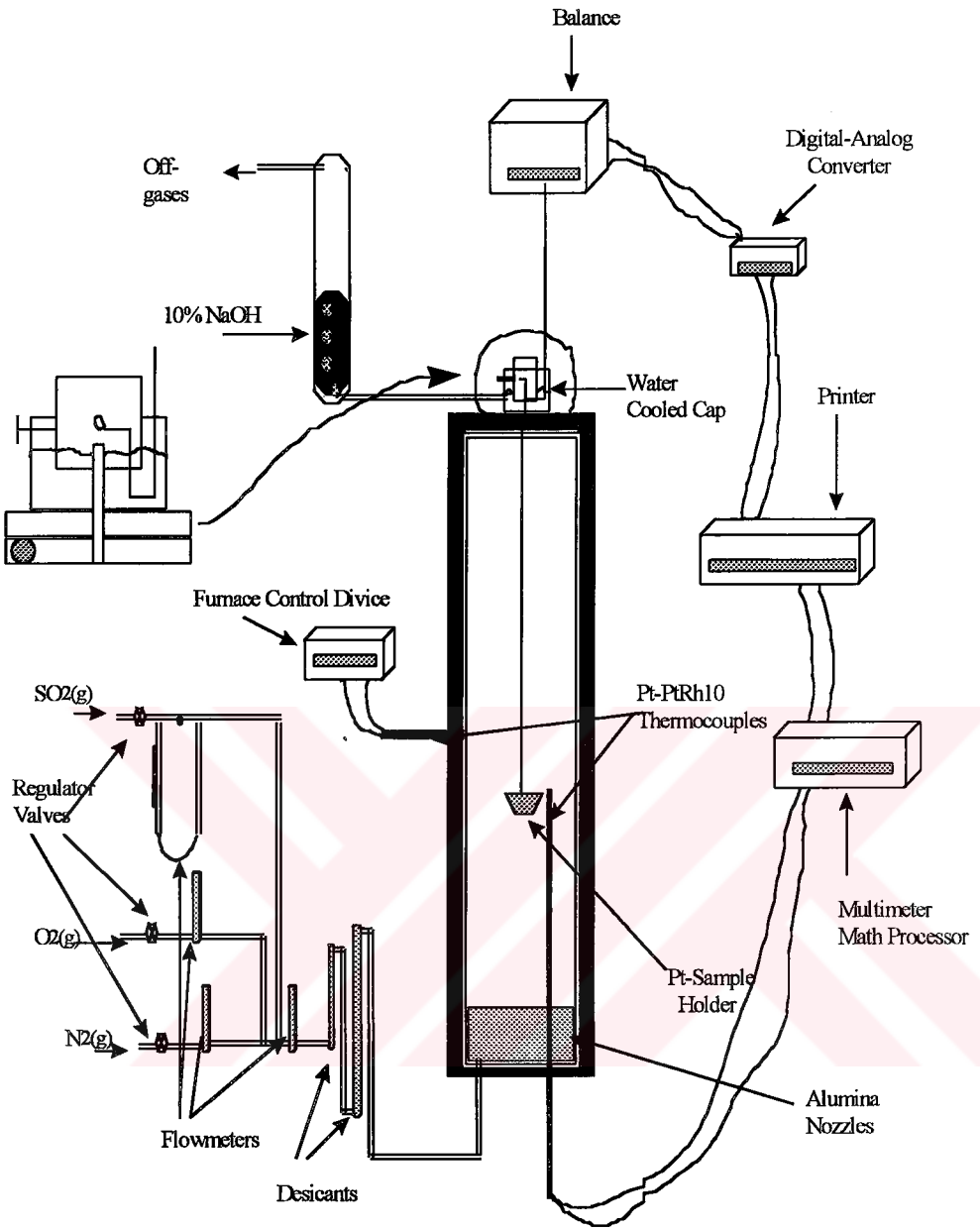

Figure 6-2. Schematic Diagram of the Experimental System.

Limestone was placed in a platinum crucible to the hottest zone of the furnace and hung from the balance by a platinum rod. Platinum rod has been divided into two groups: One is coming out of the furnace and placed inside the oil-cap and the other part which is coming from the balance system and connecting to the other via a "J" junction. So that, it could be hung freely and not touched any of the equipment. Furnace atmosphere has been isolated by an oil pot

and a cap over the pot. Platinum rod has been place between cap and hole through the furnace. Cap fixed to the side of the pot.

6.1.3 Analytical Methods

Chemical analyzes and BET surface area measurements were used to characterize the limestone before being used in the experiments. Surface area measurements were taken using a liquid nitrogen Micro Meritics Ins. Corp. Flowsorb II model BET analyzer. Also SEM photographs were taken to determine surface characteristics.

During the experiments, the TGA method was used to record the weight change of limestone. TGA records were used to calculate conversion ratio of sulfate to oxide as a function of time and temperature change. After reactions were completed, SO_2 and O_2 flow have been cut-down and furnace cooled to the room temperature under N_2 atmosphere. Samples were immediately divided into three groups for further analyses and stored in a desiccator account for the high hydroscobic behavior of CaO.

The reacted samples were separated for SEM, x-ray and chemical analyses. Chemical analyses of calcium and magnesium were made using a flame technique by Varian Techtron, Spectr. AA 300-400 model atomic absorption spectrophotometer. Sulfur analyses were taken by Leco Corp. made CS-244 carbon-sulfur determinator. SO_4 were analyzed using wet chemical-ionchromatic method by Waters Millipore Corp. ILC-2 model analyzer. X-ray and chemical analyses were carried out at the Outokumpu Research Center in Pori, Finland. According to characteristics of the sample, x-ray analyses were taken from bottom, middle and top of the sample. X-ray analyses were performed using a Siemens AG made D-500 model x-ray diffractometer. Perception of the phases according to x-ray analyses, have given the idea of the reaction mechanisms which are possible for sulfation at the high temperatures. Combining chemical and x-ray analyses made it possible to determine exact ratio of sulfates to oxides.

In addition to chemical and x-ray analyses, cross-sections of the reacted materials were prepared using fine-grinding sand-paper and diamond paste with an ethanol–lubricant mixture. After polishing, samples were coated using a Balzers Union made SCD 640 Model coating machine. A very thin gold layer was applied due to its effect on the analyses which were taken by Noran made Voyager model Energy Dispersive X-Ray Spectrometer (EDS).

EDS analyses were taken as spot, area and line analyses to determine characteristic properties of a photographed particle. Element mapping facilities of the EDS were also used to visualize product layers of the cross-sections.

Besides the SEM studies, cross-section samples were also examined using an Olympus PMG3 model light microscope. After preparation, the cross-section samples were etched by an alkaline indicator phenolphthalein solution. Etched samples were also used to visualize boundaries of the sulfates and oxides.

SEM-EDS and light microscope studies were carried-out at Helsinki University of Technolgy, Laboratory of Materials Science and Powder Metallurgy, Espoo, Finland.

6.2. EXPERIMENTAL RESULTS AND DISCUSSIONS

A thermogravimetric balance system (TGA) was used for collecting data both from samples and furnace. TGA records from samples have been collected during experiments as weight change by time. Weight change records were then converted to $CaSO_4/CaO$ ratio.

As a starting point, limestone has been weighted and placed in a platinum crucible which was 15 mm in diameter and 11 mm in height. The crucible was then lined out to the balance system. When the crucible had been suspended freely, the sealing equipment was placed at the top of the furnace and the gas

mixture of the SO_2, O_2 and N_2 were injected. Approximately 15 minutes after the correct reaction atmosphere had been achieved, the furnace has heated up and held at the reaction temperature.

During the heating period, calcination reaction of limestone was recorded around 750°C. Calcination of limestone was completed in 30 min. As soon as calcination was completed, sulfation reactions begun to take place whilst the furnace temperature increased to approximately 900°C.

The effect of the bed thickness on diffusion of the reaction gases was determined for particle fraction between +53-75 μm. To determine the effect of bed thickness, the holder was filled with limestone be depths of 3, 6 and 10 mm. Results of these experiments can be seen in Figure 6-3.

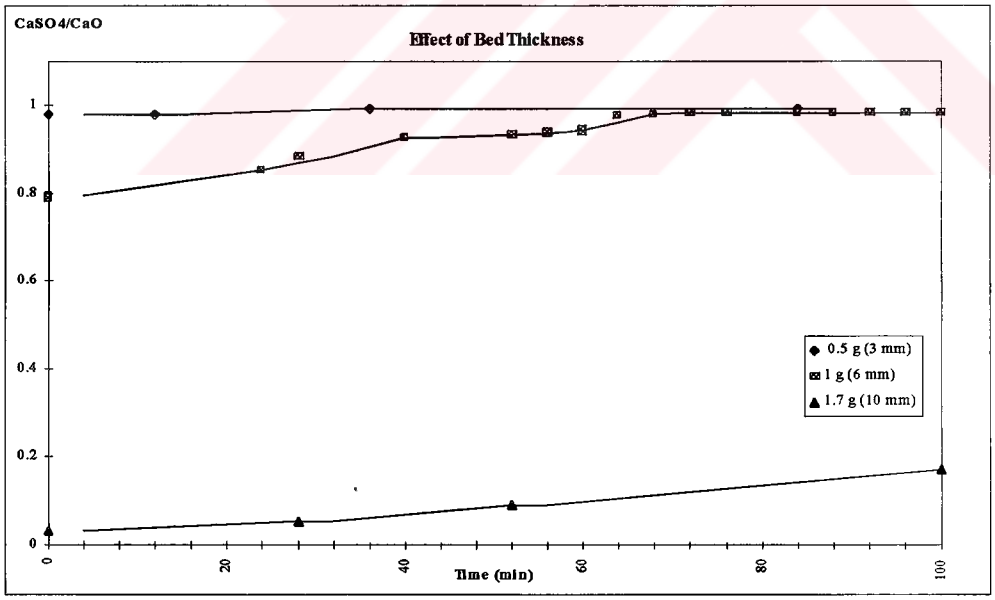

Figure 6-3. Effect of the Bed Thickness on Sulfation Ratio in Atmosphere Type 1 (10% SO_2, 70% O_2, 20% N_2) at 1200°C.

As can be seen from Figure 6-1, bed thickness of 3 mm and 6 mm gave the highest $CaSO_4/CaO$ ratio. Almost 100% of sulfation has been attained for these samples. X-ray analyses were taken from these samples showed that CaO totally sulfated to $CaSO_4$. The sulfation reaction for the 3 mm bed thickness was completed before the furnace temperature reached to the experimental temperature. The sample with 6 mm bed thickness has reached 80 % sulfation just before the furnace temperature was 1200°C. Sulfation of the sample was completed within 1 hour at the experiment temperature. Sulfation rate of the sample with 10 mm thickness in the crucible had very slow reaction rate and had reached 20 % after 1 h 40 min at the experimental temperature. Samples with 3 and 6 mm bed thickness were found sufficient enough for achieving effective sulfation ratio. In the following experiments 1.000 g (6 mm) of limestone was used to ensure enough amount of material for further analyses.

Once the amount of limestone had been chosen, experiments were carried out in the three different atmospheres given in Table 6-3. Sulfation characteristics of 4 particle fractions were also studied in each atmosphere. Effects of each atmosphere type on the particle fractions can be seen in Figure 6-4.

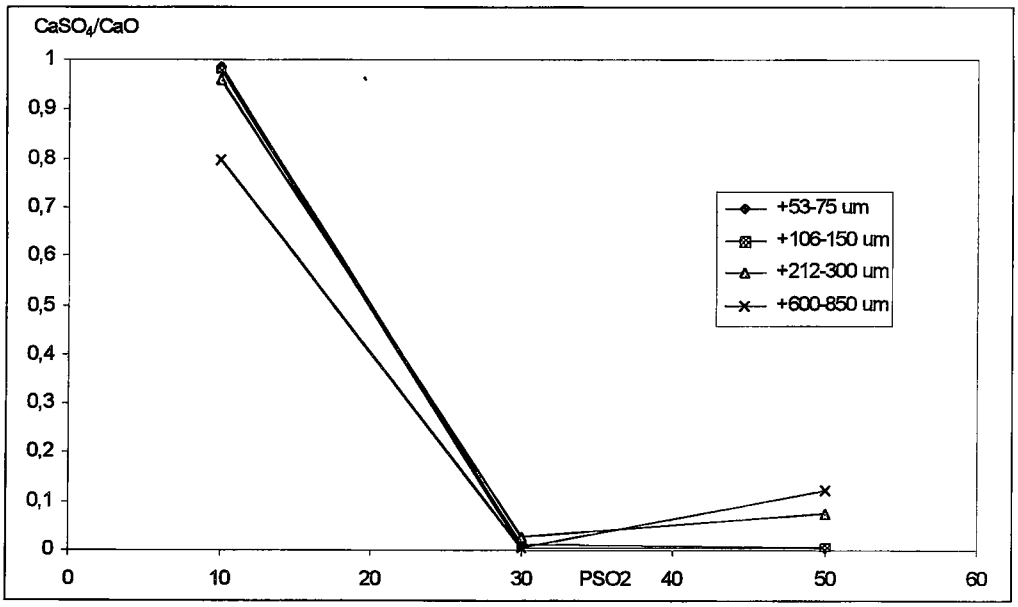

Figure 6-4. Effect of Partial Pressure of SO_2 on Particle Fractions at 1200°C.

The highest sulfate to oxide ratios were been attained in atmosphere type 1 (10% SO_2, 70% O_2, 20% N_2) for all particle fractions. In atmosphere type 1 three fractions produced essentially the same ratios of sulfation while the biggest particle fraction (+600-850 μm) gave only 80 % of sulfation ratio. However in the atmosphere type 2 (30 % SO_2, 10 % O_2 and 60 % N_2) all fractions were shown the same behavior producing the lowest sulfation ratio. In the atmosphere type 3 (50 % SO_2, 2 % O_2 and 48 % N_2) small particle fractions gave the lower sulfation limit while the biggest fraction produced ~10 % sulfation. This phenomena is will be explained later.

The influence of the atmosphere type 1 on the particle fractions are given in Figure 6-5 as a function of time. As can be seen, sulfation of the particles which have particle fraction +106-150 μm was finished before the furnace reached the experimental temperature. Sulfation of the particle fraction +212-300 μm was faster than that of the smallest fraction (+53-75 μm) at the beginning but later particle fraction +53-75 μm had reached a higher sulfation ratio than the

previous one. The coarsest particle fraction finally reached the sulfation ratio of 80 %. This results indicate the optimum pore density to particle diameter ratio. Small particle fractions showed denser structure than the coarser ones in the crucible. In these conditions, gas penetration through the pores becomes more dominant than gas diffusion either into the particle or to product layer. In this situation results suggests that the optimum pore to particle diameter value is attained by particles with +106-150 μm particle fraction. In the atmosphere type 3 which has the highest SO_2 and the lowest O_2 content this behavior is turning to reverse order. Once the sulfation reactions have started, as explained above, bed material is behaves as one particle for small particle fractions and in this manner SO_2 has to diffuse through the surface of the bed to the bottom via a sintered non-porous product layer. On the other hand, pore plugging of the whole bed was attained at higher sulfation ratio with coarser fraction than with finer ones. So that, a relatively higher sulfation ratio was attained with coarser particles.

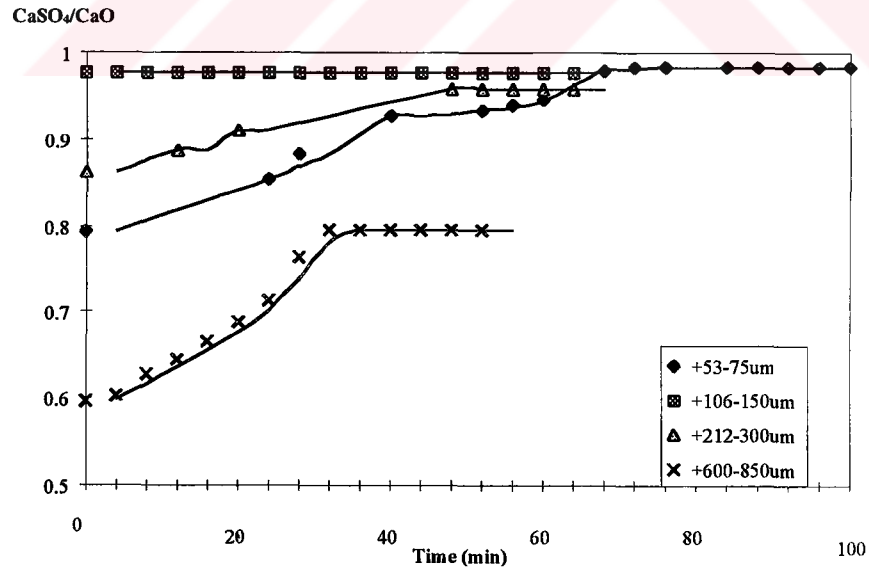

Figure 6-5. Sulfation Ratio of limestone in Atmosphere Type 1.

In addition to pore plugging phenomena, the influence of different atmospheres dictate the sulfation degree. Oxidizing characteristics of the atmosphere type 1 have given the higher sulfation ratio. On the other hand, lower sulfation ratio with atmosphere types 2 and 3 were mainly caused by the reductive characteristics. As suggested by literature [22-23] by increasing temperature under reductive atmosphere, sulfur capture of the CaO shifts to sulfur release from the particles. Under oxidizing conditions, $CaSO_4$ is a stable sulfation product whereas CaS is stable under reducing conditions. This phenomena has been discussed extensively in Section 5.1.2.

Higher sulfation ratios under atmosphere type 3 rather than atmosphere 2 can be explained by the following approach. Oxidation of SO_2 to SO_3 takes place before being reacted with calcium particles. After this stage, diffusion of the SO_3 becomes the controlling parameter for further sulfation reactions either into pores or to the product layer. In this sense, higher O_2 concentrations causes more rapid sulfation reactions and the formation of $CaSO_4$ sets-up diffusion barriers on the rate of SO_3 penetration. In summary, high O_2 concentrations infers high SO_3 concentrations at the edge of the particles which causes faster pore plugging of the whole system and quicker cessation of the absorption. It was suggested [9] that increasing O_2 concentration tended to provide lower sulfation conversion.

In the experiments in atmosphere types 2 and 3, limestone was sulfated slightly on the surface of the bed. The diffusion of the both SO_2 and O_2 is inhibited by this dense and non-porous product layer. The product layer of the calcined limestone can been seen in Figure 6-6.

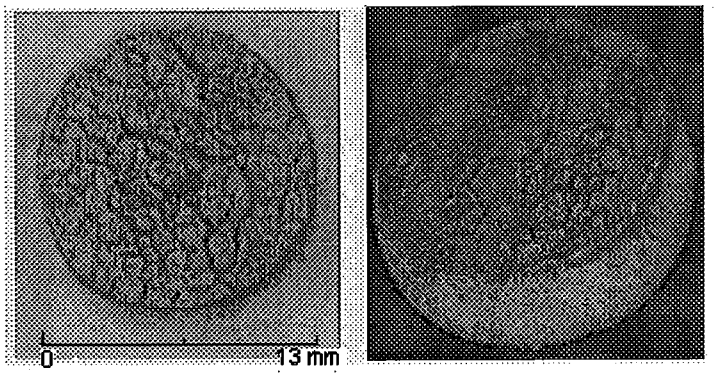

Figure 6-6. Calcined and Slightly Sulfated Limestone Particle Fraction +53-75μm. Atmosphere Type 2 at 1200°C ~ 2 h 40 m

In experiments which were carried out in the atmosphere types 2 and 3, final $CaSO_4/CaO$ ratios were not more than 0.1. During the experiments, TGA records showed that sulfation was also taken place at temperatures lower than 1100°C but after the temperature exceeded 1100°C decomposition of already sulfated particles became significant. Finally, reactions in the furnace were ceased with sulfation ratio of around 0.1. This effect on the particle fraction +212-300 μm can seen in Figure 6-7.

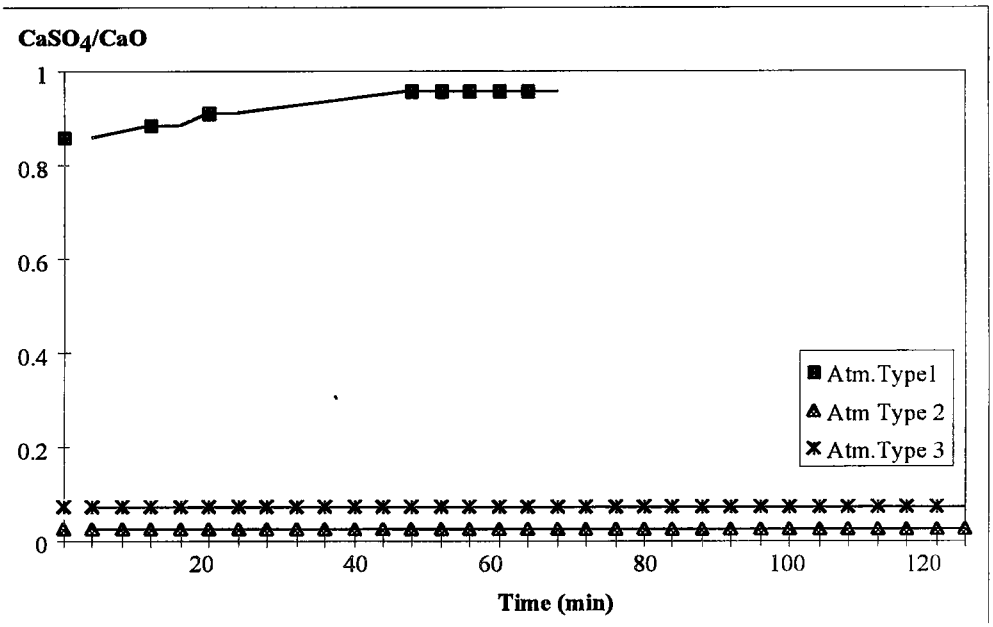

Figure 6-7. Effect of the Different Atmospheres on the Particle Fraction +212-300μm at 1200°C.

Particles which were partly sulfated were examined using different analytical methods. Besides the X-ray and chemical analyses, the SEM-EDS combination were used for analyzing all reacted particles. SEM-EDS studies were based on cross-section samples of the particles. The cross-section samples were pictured and analyzed after polishing and coating by gold. Three different methods were used for analyzing the particles. Spot analyzes mainly were used for the particles which the x–ray results gave a $CaSO_4$ phase only. Line analyses and element mapping facilities were used particles which have lower conversion ratios. Figure 6-8 shows results from the different analytical methods.

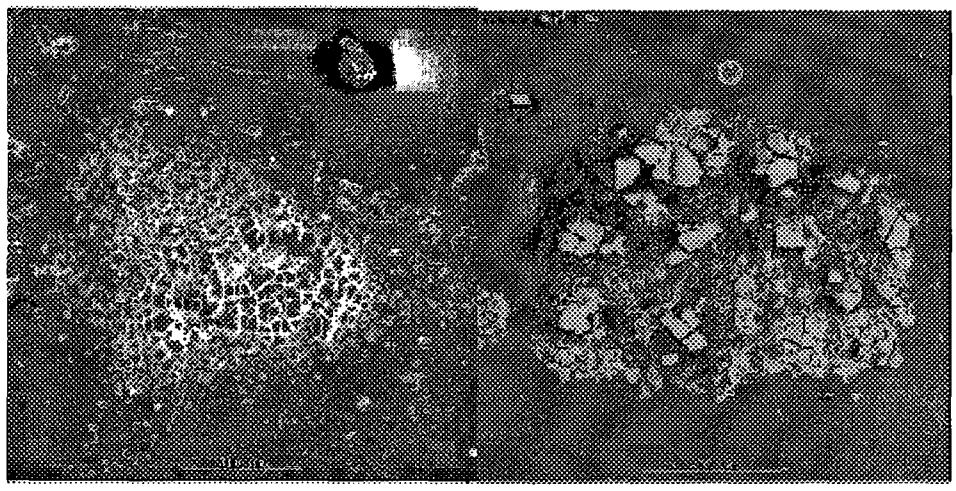

(a) (b)

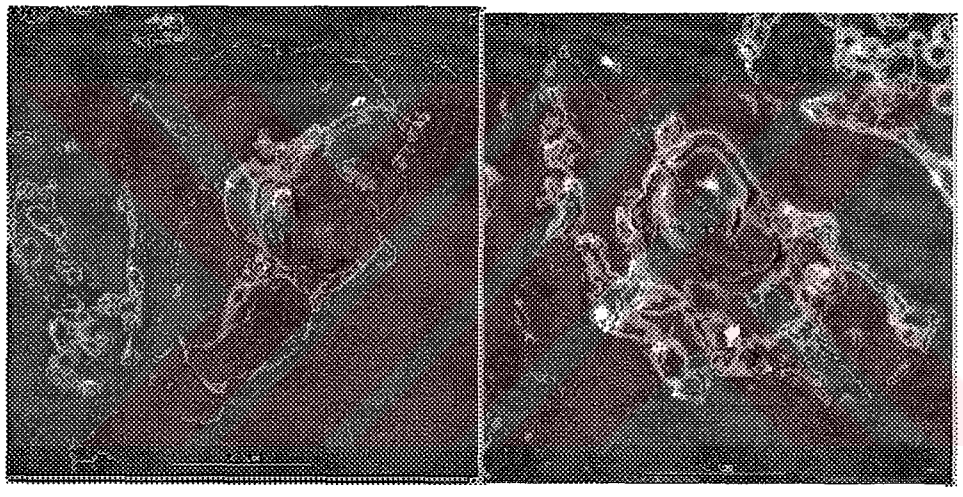

(c) (d)

Figure 6-8. Partially Sulfated Limestones.

Above figures show the samples that were reacted in the different atmosphere types at different particle fractions. Figure (a) was reacted in the atmosphere type 1 (10% SO_2, 70% O_2, 20% N_2) and original particle fraction was +600-850 μm. X-ray analyses were determined two different phases, mainly $CaSO_4$ and CaO (***Mg- components for all reacted samples were only present as MgO.***). Element mapping facilities of EDS was used to analyze the particle. The

result showed element distribution of Ca, S and O that white area in the middle of the particle is contains Ca and O. This sample has an overall 0.796 $CaSO_4$/CaO ratio.

The particle shown in Figure (b) had an initial particle size of +53-75 μm and was reacted in the atmosphere type 3 (50% SO_2, 2%O_2, 48 N_2). The Figure shows that particles were sintered during the reactions. X-ray analyses were indicated that particle contains also CaS and CaO in addition to $CaSO_4$. EDS analyses were taken as spot analysis. According to EDS results points, 1 and 2 were in CaO form while the background contains both CaS and $CaSO_4$. This sample had 0.0041 $CaSO_4$/CaO ratio when the experiments were completed.

Figures (c) and (d) have been taken from same particle fraction which was +106-150 μm. X-ray analyses showed that particle contains CaO, CaS and $CaSO_4$ as Figure (b). This particle was reacted in the atmosphere type 2 (30% SO_2, 10% O_2, 60% N_2) and has 0.0041 $CaSO_4$/CaO ratio. Line analysis which was taken from figure (d) suggested that the blocked core contains CaO while the crust was CaS and $CaSO_4$. Figure (c) was analyzed using spot analysis method which CaO detected at the edge of the hole.

In the atmosphere types 2 and 3 the sulfation continued during the cooling down period under N_2 protection. So, these figures which were shown here actually have higher sulfation ratios. This effect is due to the thermodynamic behavior of the $CaSO_4$ and CaS. Temperature decrease was allowed further reactions of residue SO_2 and O_2 which were remaining in the furnace atmosphere. Because of this effect, figure (b) has 0.277 conversion ratio while figures (c) and (d) have 0.36 final conversion ratio after cooling down the furnace to room temperature. According to this observation, reaction shift for high temperatures should be considered again for discussing the results from analyses. This phenomena is also mainly caused by reactions between SO_2 and O_2 before being reacted with the sample. Temperature decrease favors further oxidation of CaS even at low oxygen pressures. Furthermore, around 700°C the oxidation of SO_2 is

also takes place again and by force of these factors excess sulfation of the sample can not be prevented.

After SEM-EDS studies, samples were studied using light microscope. The aim of the this study was to visualize boundary layers of the reacted surface and unreacted CaO. For this purpose an alkaline indicator phenolphthalein was used because of basic characteristic of the CaO. Phenolphthalein solution was etched on the surface of the polished cross-section samples. Samples with high sulfation efficiency were not showed any changes by phenolphthalein. These samples were also given only $CaSO_4$ phase by x-ray diffractometer. Samples which were low sulfation efficiencies and also CaO phase determined by x-ray analyzer, changed color from white to red. These figures can be seen in Figure 6-9.

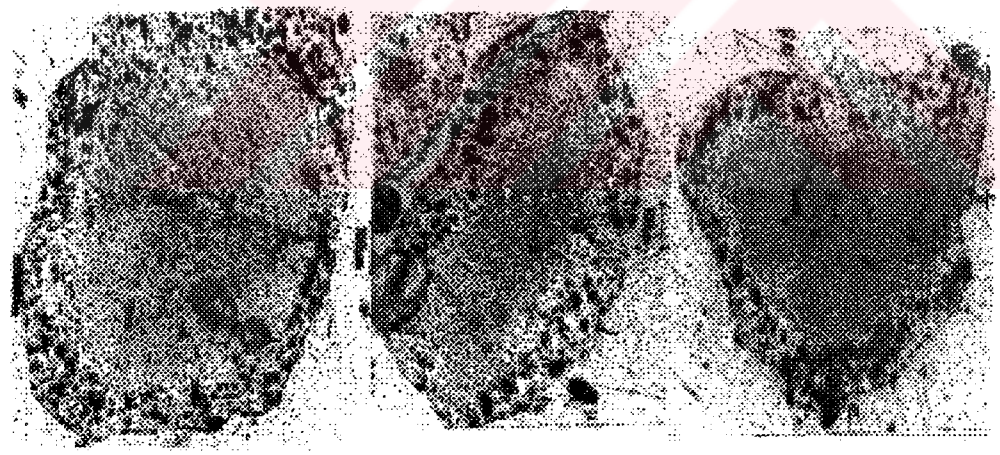

Figure 6-9. Particles etched by phenolphthalein solution.

Original particle size +650-850 μm reacted in the Atmosphere type 1, same conditions with Figure 6-8 (a). Red areas in the middle of the each particle suggests unreacted CaO meanwhile areas outside are suggests acidic $CaSO_4$.

Overall results from the experiments are given in Table 6-4. As can be seen from the X–ray analyses, $CaSO_4$ is the stable product as long as oxidizing conditions are ensured in the furnace. When the conditions were turned to reducing atmospheres, reaction products also consist of CaS. Mg components kept their inert behavior as it was suggested in the literature [9,17] regardless of the atmosphere type.

Table 6-4. General Chemical and X-ray Analyses

Particle Size	Atmosphere Type	Input	Output	CaSO4/CaO	Ca	Mg	SiO2	SO4	S	X-Ray
+53-75μm	10%SO2, 70%O2, 20%N2	1.000	1.305	0.98	28.08	0.53	1.1	74.9	23.5	CaSO4, MgO
+53-75 μm	10%SO2, 70%O2, 20%N2	1.669	1.187	0.17	50.71	0.98	2	22.2	8.2	CaO, CaSO4, MgO
+53-75 μm	10%SO2, 70%O2, 20%N2	0.509	0.667	0.99	27.28	0.54	1.2	76.3	21.9	CaSO4, MgO
+106-150μm	10%SO2, 70%O2, 20%N2	1	1.3	0.98	27.65	0.37	0.94	75.2	23.6	CaSO4, MgO
+212-300 μm	10%SO2, 70%O2, 20%N2	1	1.286	0.96	29.3	0.44	1.1	76	24.6	CaSO4, MgO
+600-850μm	10%SO2, 70%O2, 20%N2	1	1.168	0.8	30.8	0.46	1.2	66	22	CaSO4-CaO
+53-75 μm	30%SO2, 10%O2, 60%N2	1	0.595	0.011	50.4	0.94	1.9	35	11.3	CaO-CaSO4-CaS-MgO
+106-150 μm	30%SO2, 10%O2, 60%N2	1	0.59	0.0041	51	0.65	1.7	7	5.3	CaO-CaSO4-CaS-MgO
+212-300 μm	30%SO2, 10%O2, 60%N2	1	0.59	0.0041	46.9	0.78	1.9	40	13.1	CaO-CaSO4-CaS-MgO
+600-850 μm	30%SO2, 10%O2, 60%N2	1	0.59	0.0041	45.2	0.85	2	42	13.1	CaO-CaSO4-CaS-MgO
+53-75μm	50%SO2, 2%O2, 48%N2	1	0.59	0.0041	45.9	0.95	1.9	35	11.9	CaO-CaSO4-CaS-MgO
+106-150μm	50%SO2, 2%O2, 48%N2	1	0.59	0.0041	60.9	0.81	1.9	12.8	4.2	CaO-CaSO4-MgO
+212-300 μm	50%SO2, 2%O2, 48%N2	1	0.64	0.073	55	0.92	2.2	20	6.4	CaO-CaS-CaSO4-MgO
+600-850 μm	50%SO2, 2%O2, 48%N2	1	0.676	0.122	53.3	0.85	1.8	37	12.3	CaO-CaS-CaSO4-MgO

Analyses taken from samples of the atmosphere type 2 and 3 were given as final analysis which includes excessive sulfation during the cooling period. $CaSO_4$/CaO ratios of all the samples are given as instantaneous conversion ratio at the time when the experiments were halted.

6.3. REACTION KINETICS OF HIGH TEMPERATURE SULFATION OF LIMESTONE

Shrinking core model (Figure 6-10) was used for calculating kinetic parameters with following assumptions:

i. Temperature of the particles is as same as gas temperature in the furnace.

ii. Greater than 30 % of the sulfation had been completed in the first 2 minutes.

iii. Average particle diameter of 64 μm was used and particles were assumed to be spherical in shape.

iv. Particles were in straight order in the layers and surface area was calculated from half of the particles.

v. After this initial period, the rest of the calculations were based on one particle layer of CaO.

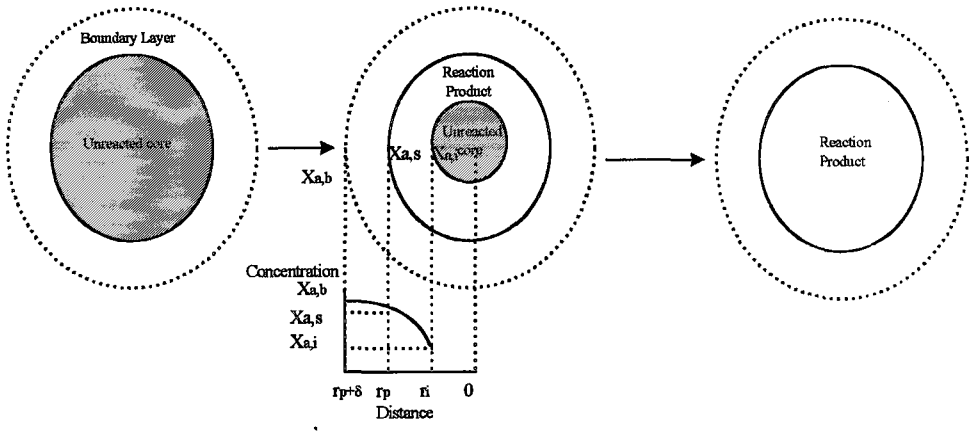

Figure 6-10. Schematic Diagram of the Shrinking Core Model [25]

The model was applied to particle fraction of 53-75 μm. These particles were reacted in atmosphere type 1 (10 % SO_2, 70 % O_2 and 20 % N_2) with 0.98 $CaSO_4$ to CaO conversion ratio. During the heating-up period, the sample first calcined from $CaCO_3$ to CaO and then sulfation reactions began. Reaction 5.2 is the overall sulfation reaction for the model. The rate of the sulfation was high in the initial stage, but after a time decreased gradually as the sulfation proceeds. The initial rapid reaction results from the higher surface area of unsulfated CaO. The rate decrease was due to both the surface area loss and to the build up of a continuously growing product $CaSO_4$ layer on the surface of unreacted CaO. Figure 6-11 shows the weight and temperature changes with time during the experimental period.

$$CaO_{(s)} + SO_{2(g)} + \tfrac{1}{2}\, O_{2(g)} \rightarrow CaSO_{4(s)} \qquad (5.2)$$

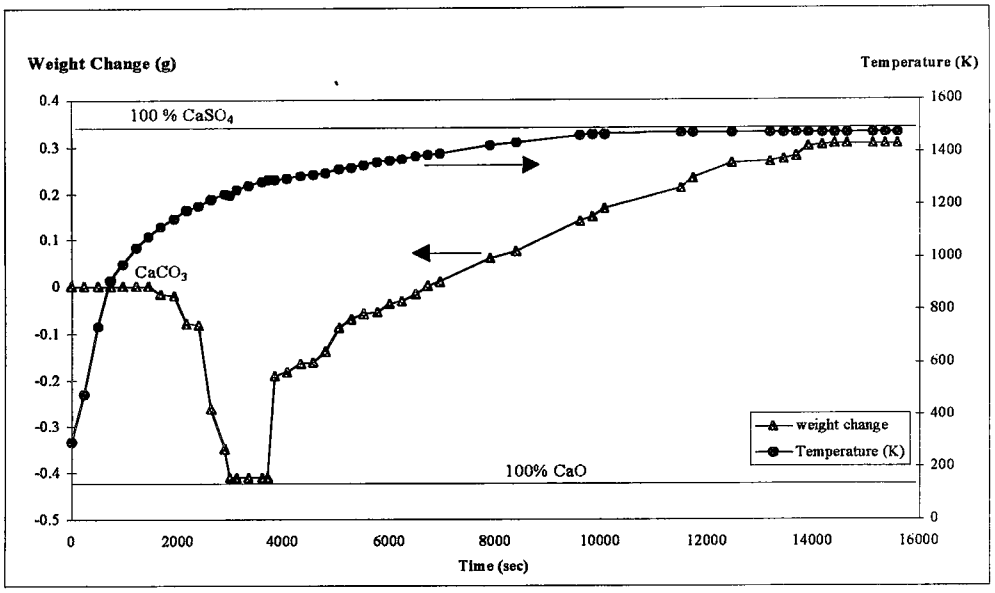

Figure 6-11. Weight and Temperature Changes with Time

TGA records were used for kinetic calculations. Data from records have been corrected according to chemical analyses of the limestone. Calculations were performed using results measured after the first two minutes of reaction with SO_2. Figure 6-12 shows mass change per second versus the temperature increase during the sulfation proceed.

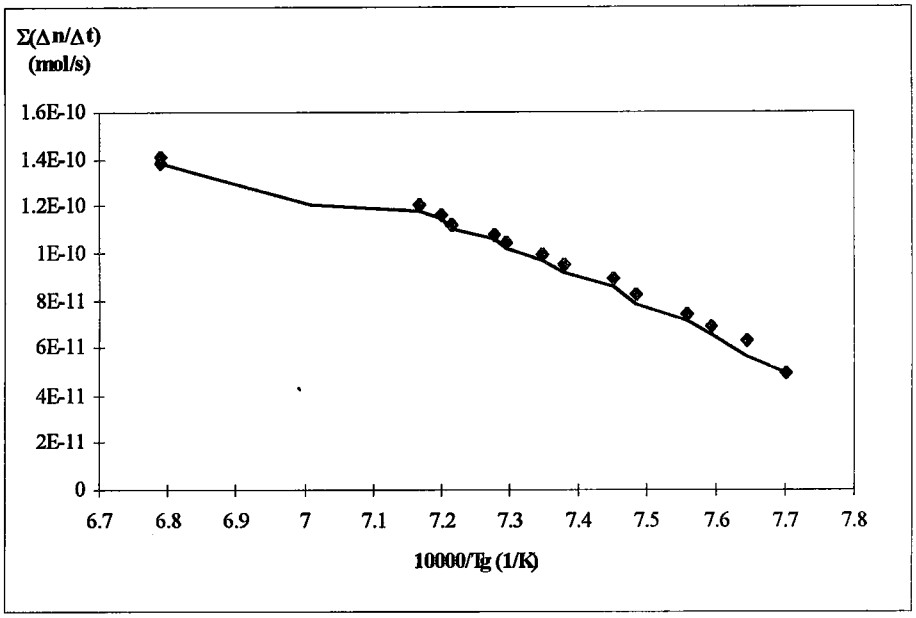

Figure 6-12. Mass change per second by Temperature.

Once the mass change was calculated for the one particle layer, the overall reaction rate was calculated for each step using equation (6.1) according to reaction (5.2)[23]. The kinetic model was based on the SO_2 consumption per second because of its direct effect on the overall reaction rate.

$$\frac{\Delta n_{SO_2}}{\Delta t} = C_{SO_2} A_{reaction} k_{ov} \qquad (6.1)$$

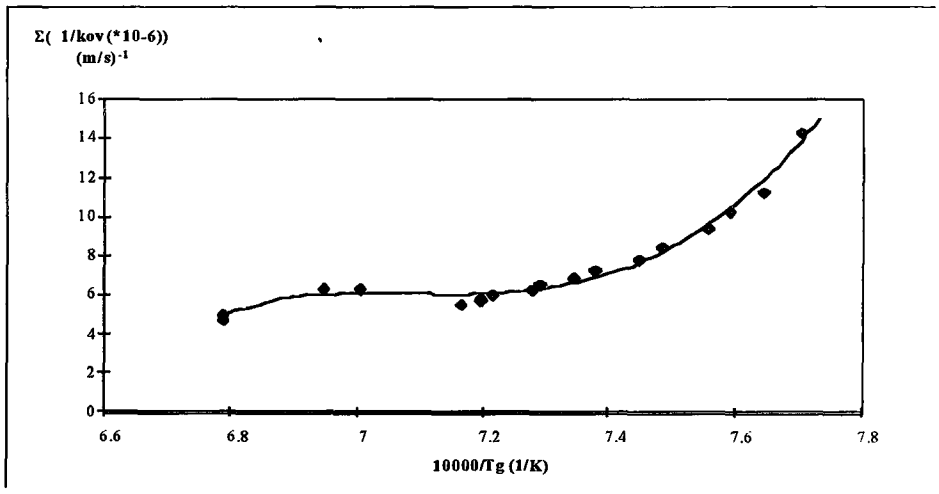

Figure 6-13. Cumulative Overall Reaction Rate of the Sulfation Process

Cumulative overall reaction rate change can be seen from Figure 6-13. As slope of the overall reaction rate curve suggests the reaction rate increases with increases in temperature. This effect has mainly been caused by the pore plugging phenomena caused by reaction product. Pore plugging has occurred either by sintering of the particles or by reaction products which are blocking the diffusion of the reaction gases through to boundary layer. When the later mechanism is dominant, sulfation occurs by solid-state diffusion.

CHAPTER 7

CONCLUSIONS AND RECOMENDATIONS

Sulfation of limestone was studied using a thermogravimetric balance system in a vertical furnace. The effect of different atmosphere types was examined according to flash smelting furnace reaction shaft conditions at 1200°C.

Sulfation of limestone was attained as long as oxidizing conditions were ensured during the experiments. When relatively reductive atmospheres were used, sulfation of limestone was ceased at lower percentages involving more complex routes and mechanisms. As can be seen from Figure 7.1 increase in temperature have a negative effect on sulfation.

It was observed that sulfation had taken place below 1100°C but decomposition of already sulfated particles was begun with increasing furnace temperature at the atmosphere types 2 (30 % SO_2, 10 % O_2, 60 % N_2) and 3 (50 % SO_2, 2 % O_2, 48 % N_2)

Kinetic calculations suggests that initial sulfation occurs very rapidly. Initial stage of sulfation was completed in ~2 minutes with approximately 30 % sulfation for the atmosphere type 1 (10 % SO_2, 70 % O_2, 20 % N_2). This stage was controlled by chemical reaction rate. Arrhenius type equation (6.3) was used to define parameters of this step but in this case relatively high concentrations caused more rapid reaction than the literature suggests. It was impossible to

calculate the rate of this initial step. After this stage, diffusion of the reaction gases has been controlling parameter for rest of the sulfation. As it was suggested by Figures 6.14 and 6.15, solid-state diffusion was become the controlling step due to pore plugging of the system.

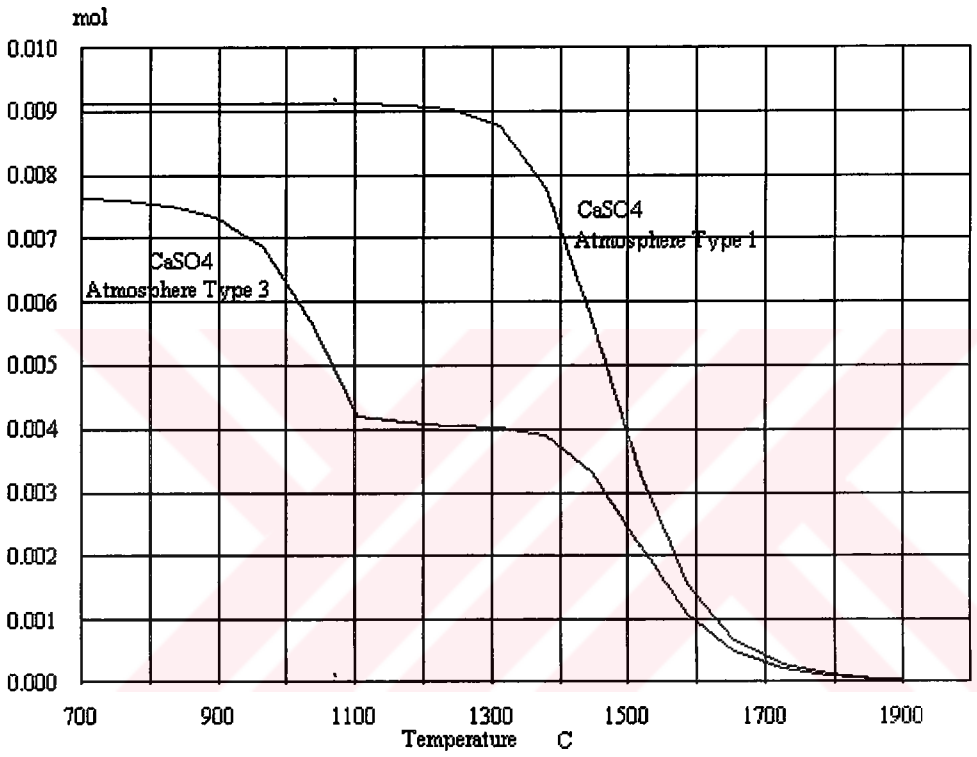

Figure 7-1. Equilibrium Composition of $CaSO_4$ [24]

For future studies of the subject following recommendations can be considered:

i. Experimental equipments should be selected carefully for study of high sulfur concentrations. Gas carriage tubes and injection system should be resistant to SO_2. In this study, plastic tubes and connectors have been used as gas transport equipment at the beginning. After a while, plastic materials in the construction of experimental system have begun to react with SO_2.

ii. Humidity in the system should be carefully controlled and be avoided as it forms sulfuric acid with SO_2 and O_2 and corrodes the metallic constructions such as valves and regulators. System should be checked regularly to avoid any leakage of SO_2.

iii. Uptake gases should be neutralized and environmental safety regulations should be checked according to allowance of SO_2 or its compounds.

iv. Special attention should also be paid for storing and preparing of the samples due to hydroscobic characteristic of CaO. Polishing of the cross-section samples should be made by alcohol mixtures and polishing materials and methods should be chosen by extreme passion. Toughness of Ca components made proper polishing difficult.

REFERENCES

[1] **BOYNTON, R.S.,** Chemistry and Technology of Lime and Limestone, Interscience Publishers, USA, (1966).

[2] **SAVIN, I.** Theory of Metallurgical Processes, Pyrometallurgical Processes", 2nd Edition, Mir Publishers, Moscow, USSR, (1978), pp81-82.

[3] **ROSENQVIST, T.,** Principles of Extractive Metallurgy, McCraw Hill, (1974), pp.337-338.

[4] **GILCHRIST, J.D.** Extraction Metallurgy 2nd Edition., Biddles, London, .210-219.

[5] **KEMORI, N., DENHOLM, W.T. and KUROKAWA, H.,** Reaction Mechanism in a Copper Flash Smelting Furnace, Metallurgical Transactions B, Vol. 20B, (1989) pp.327-336.

[6] **JOKILAAKSO, A., HOKAINEN, A., TEPPO, O., YANG, Y., LILIUS, K.,** Experimental and Computational Fluid Dynamics Simulation of the Outokumpu Flash Smelting Process, Mineral Processing and Extractive Metallurgy Review, Vol.15,(1995), pp.217-234.

[7] **DAVENPORT, W.G., PARTELPOEG, E.H.,** "Flash Smelting Analysis, Control and Optimization", 1st Edition, Pergamon Press, New York, (1987), pp.1-35.

[8] **NERMES E.** R&D on Flash Smelting, Flash Smelting Symposium, Salvador, (1980), pp.82-109.

[9] **BURDETT, N.A.**, The inhibition of the Limestone Sulfation Process During Fluidised Bed Combustion –A Theoretical Approach, Journal of the Inst. Of Energy, 198, (1983), pp.198-208.

[10] **DAM-JOHANSEN, K., HANSEN, P.F.B., OSTERGAARD, K.**, High Temperature Reaction Between SO_2 and Limestone — III. A Grain — Micrograin Model and Its Verifications, Chemical Engineering Science, Vol.46, No.3, (1991), pp.847-853.

[11] **DENNIS, J.S., and HAYHURST, A.N.**, Mechanism of the Sulfation of Calcined Limestone Particles in Combustion Gases, Chem. Eng. Sci., Vol.45, No. 5, (1990), pp. 1175-1187.

[12] **Borgwardt, R.H. and Harvery, R.H.**, Properties of Carbonate Rocks Related to SO_2 Reactivity, Environmental Science & Technology, Vol. 6, No.4, (1972), pp-350-360.

[13] **HU, N. and SCARONI A.W.**, Calcination of Pulverized Limestone Particles Under Furnace Injection Conditions, Fuel, Vol.75 No.2 (1996), pp.177-186.

[14] **SILCOX, G:D., KORAMLICH, J.C. and PERSHING, D.W.**, A Mathematical Model for the Flash Calcination of Dispersed $CaCO_3$ and $Ca(OH)_2$ Particles, Ind. Eng. Chem. Res., Vol.28, (1989), pp.155-160.

[15] **Campbell, F.R., Hills, A.W.D., Paulin, A.**, Transport Properties of Porous Lime and Their Influence on the Decomposition of Porous Compacts of Calcium Carbonate, Chem. Eng. Sci., Vol. 25, (1970), pp. 929-942.

[16] **WARREN, G.**, Sulfur Fixation at High Temperature with in the Copper Smelting Process, The Minerals, Metals & Materials Society, EPD Congress, (1996), pp.785-797.

[17] **HARTMAN, M. and COUGHLIN, R.W.**, Reaction of Sulfur Dioxide with Limestone and the Influence of Pore Structure, Ind. Eng. Chem., Process Des. Develop., Vol. 13, (1974),No. 3, pp. 248-253.

[18] ALVFONDS, P. and SVEDBERG, G., Modeling of the Sulfation of Calcined Limestone and Dolomite – A Gas Solid Reaction with Structural Changes in the Presence of Inert Solids, Chem. Eng. Sci. Vol.43, No.5, (1988), pp.1183-1193.

[19] HARTMAN, M., Grain Model for the Reaction of SO_2 with Limestone, Chem. Reac. Eng. Vol.1, Frankfurt, (1976), pp.214-221.

[20] SNOW, M., LONGWELD, J., and SAROFIM, A., Direct Sulfation of Calcium Carbonate, Ind. Eng. Chem. Res., Vol. 27, (1988), pp.268-273.

[21] CAVANAGH, R. and WARNER, N.A., Reaction of High Strength Sulfur Dioxide with Limestone and Dolomite at Elevated Temperature, EPD Congress, (1996), .pp.809-824.

[22] LYNGFELT, A. and LECKNER, B., SO_2 Capture in Fluidised–Bed Boilers: Re–Emission of SO_2 Due to Reduction of $CaSO_4$, Chem. Eng. Sci., Vol.44, No.2, (1989), pp. 207-213.

[23] LYNGFELT, A. and LECKNER, B., Sulfur Capture in Fluidised–Bed Boilers: The Effect of Reductive Decomposition of $CaSO_4$, The Chem. Eng. Jour., Vol.40, (1989), pp.59-69.

[24] HSC

[25] GEANKOPLIS, C.J., Mass Transport Phenomena, Ohio State University, Columbus Ohio, (1972).

CURRICULUM VITAE

Özgür Bilinç YILMAZ was born in 1973 in Kayseri, Turkey. He completed his high school education in Sümer Lisesi Kayseri. He enrolled Istanbul Technical University (ITU) in 1991. He was graduated from Language and History Department of ITU, English Language Program in 1992 and continued his education in the Faculty of Chemical and Metallurgical Engineering at the Department of Metallurgical Engineering. He was graduated as a Metallurgical Engineer (B.Sc.) in 1996. After his graduation, he was continued his education in the Institute of Science and Technology, Department of Metallurgical Engineering at ITU.

He completed his Bachelor Thesis on "Extraction of Lead and Zinc from Neutral Leach Residues".

He completed his training studies in HES Cable Factory, in 1993 and Erciyas Pipe Manufacturing Factory in 1994.

He was employed as a summer trainee by Outokumpu Research Center in 1995 and 1996. During his employment he produced two literature review on Flash Smelting Processes of Lead and High Temperature Reactions of Limestone in SO_2–rich Atmospheres.

He studied at Helsinki University of Technology as a guest student in 1997-1998.

He has a published paper titled "***Extraction of Lead and Zinc from the Neutral Leach Residues of CINKUR***" in Metallurgy, 101 pp.25-31, April,1996 a publication of UCTEA Chamber of Metallurgical Engineers.